SEASONAL CLOUDINESS AND CLOUD WATER PATH FROM ISCCP C2 DATA

Frances Drake

WORKING PAPER 91/6

SCHOOL OF GEOGRAPHY • UNIVERSITY OF LEEDS

Seasonal Cloudiness and Cloud Water Path from ISCCP C2 Data

WORKING PAPER 91/6

Frances Drake

School of Geography,

University of Leeds,

Leeds, LS2 9JT,

United Kingdom.

Telephone 0532 333332

Fax 0532 333308

Abstract

ISCCP C2 data are used to produce extreme season zonal means and global climatologies of cloud parameters for 1984. The total cloud amount, in general, agrees well with previous cloud climatologies. The main climatic features are observed, notably the equatorial maximum associated with the intertropical convergence zone, the sub-tropical minima and mid-latitude maxima. The polar regions are areas of disagreement. For both poles maximum cloudiness occurs in the winter. Antarctica is found to be an area of cloud amount minimum which agrees well with more recent surface observations. Results from the frequency of occurrence of cloud types show low clouds to be the most common cloud type over the ocean. Areas of frequently occurring low cloud are found on the west coasts of sub-tropical continents, indicating the presence of marine stratocumulus. The sub-tropical high pressure zones are areas with a very low frequency of occurrence of middle and high cloud types. The Monsoon is easily visible by an increase in the high cloud frequency of occurrence during northern hemisphere summer. The total water path results highlight the difficulties of cloud retrieval over permanent snow/ice cover. At present the water path results are unreliable.

Keywords: cloud climatologies water path layer cloud

Introduction

The International Satellite Cloud Climatology Project (ISCCP) (GARP, 1978) is a major initiative to provide the climate modelling community with a definitive and flexible cloud climatology. ISCCP provides data at three levels: radiance data globally every three hours at a 30km resolution (B3 data), cloud data globally every three hours at a nominal 250km resolution (C1 data) and monthly mean statistics of the C1 data (C2 data).

As pointed out by several authors (Slingo, 1987 and Morcrette, 1991) the validation of cloudiness as predicted by atmospheric general circulation models (AGCMs) poses many problems. Not least the differences in the definition of cloudiness by models and observations. The problems of satellite retrieved cloudiness are discussed by Rossow (1989) and the problems of surface based observations are equally well known (Malberg, 1973 and Drake, 1987). The limitations this places on the validation of cloudiness in AGCM's has led to top of the atmosphere (TOA) radiance measurements, such as those provided by Nimbus 7 and the Earth Radiation Budget Experiment, to be used extensively to validate AGCMs. Validation of model TOA radiances with observed TOA radiances removes any definitional problems but by itself is not a complete validation of the model. As pointed out by Buriez et al. (1989) such an approach does not guarantee a unique solution to the radiances and can lead to very different bottom of the atmosphere radiances. The study by Buriez et al. (1989)

also found that differences between observed and calculated TOA radiances due to differences in the cloud cover were compensated for by the different radiative properties of the observed and model clouds. Finally much climate modelling research is now directed towards the problem of the enhanced greenhouse effect. There has been growing evidence from various studies that cloud properties may change in such a carbon dioxide enriched climate, changing the radiation balance and modifying the greenhouse perturbed climate (Slingo, 1989). However as yet the full role of clouds in controlling the current climate is still far from understood.

Therefore the need to study clouds and correctly predict them in climate models is now widely recognised (Houghton et al., 1990). Cloud radiative properties are dependent on the horizontal and vertical cloud distribution, and cloud optical properties. ISCCP provides cloud distribution data, which has been available before from other surface and satellite based cloud climatologies, but ISCCP provides some of the first information, on a global scale, of cloud optical properties. The results presented are from the C2 data, in particular the zonal means of cloudiness and total water path for the extreme seasons of 1984. Total water path is compared to the UK Meterological Office results previously published by Smith (1990). The global distribution of total cloud amount, the frequency of occurrence of low, middle and high cloud and total water path are also shown.

The ISCCP C2 Data Set

As with any data set, it is important that the construction of the data set is fully understood in order for the results to be interpreted correctly. The ISCCP cloud data products and the cloud retrieval procedure are described in detail in Rossow and Schiffer (1991) and will not be discussed here. The ISCCP C2 data set is fully described in Rossow and Walker (1991), a brief summary of the averaging procedures and relevant parameters is presented in the following section.

Definition of Parameters

The C2 data is the monthly mean of the C1 data. Diurnal information is preserved by providing eight data sets, called hour-monthly means, which are the separate monthly averages of the time slots 00, 03, 06, 12, 15, 18, and 21 GMT. The ninth data set, the monthly mean, is the average of these eight hour-monthly means. The ISCCP C2 data set provides some 22 parameters of global cloud data (Table 1). In addition average surface and atmospheric properties and positional information are also given; in total 72 parameters. This paper concentrates on the total cloud amount, the frequency of occurrence of the ten cloud types and cloud water path of the monthly mean.

The total cloud amount (parameter 8) is the time average of the numbers obtained from the C1 data by dividing the number of cloudy pixels by the total number of pixels. If there were no

partially covered pixels this would be the time-averaged cloud cover fraction (p.c. Rossow, 1991). As not all the pixels from the C1 data are 100% cloud covered, parameter 8 was labelled the cloud (time) mean frequency. So in the strictest sense parameter 8 can only be quantitatively accurate when used together with the optical properties. However parameter 8 does contain many cases where the pixels are completely cloud covered. Furthermore quantitative comparisons with surface-observed cloud fractions are excellent (p.c. Rossow, 1991). So this is a reasonably accurate cloud fraction and will be referred to as total cloud amount from now on.

The ten cloud types reported are all "frequency of occurrence" but fall in to two categories. Rossow and Walker (1991) describe the cloud types as follows (Figure 1). The first category consists of three types, low, middle and high, these are defined only by cloud top pressures determined solely from the infrared radiances and are reported for day and night time conditions. The second category consists of the remaining seven types. These are determined from the cloud top pressure and optical thicknesses and are reported for daytime only. Although, strictly speaking, this second category are "radiometric" cloud types, they are given names corresponding to the classical cloud types. Rossow and Schiffer (1991) found the behaviour of the radiometric cloud type to be consistent with the classical cloud type they were named after.

As Rossow and Walker (1991) point out averaging of the C1 parameters can occur in two ways depending on the purpose. Many cloud variables are dependent on the cloud radiative properties in a non-linear way. A linear average of the C1 reported numbers would not give the true average radiative effect. Parameters such as optical thickness need a non-linear weighting scheme. All parameters in the C2 data are averaged in this way except parameter 20. Parameter 20 is called "PATH" and is a measure of the cloud water path. It is a linear average of the optical thickness values recorded in the C1 data. In retrieving the optical thicknesses a constant cloud particle size is assumed. Parameter 20 therefore can be used to estimate the mass of cloud water per unit area.

$$\text{Cloud Water Path} = 40\ r\ \text{PATH}/3\ Q\ \text{kgm}^{-2}$$

where r is the average particle radius in cm, and Q is the normalized Mie extinction efficiency at 0.6 m wavelength. For the cloud particle size distribution used r= 10^{-3} cm

$$\text{Cloud Water Path} = 6.292\ \ \text{PATH}\ \text{gm}^{-2}$$

It is this variable not PATH that is considered in this paper.

Spatial Representation of ISCCP C2 Data

In preparing zonal means from the ISCCP C2 data the spatial and radiative characteristics of the data set need to be conserved.

ISCCP data is presented on a nominal 250km square grid. The C2 data tapes containing the processed cloud data hold the data in 6596 equal area grid squares. The equal areas are arrived at by dividing the earth into 72 latitude zones. Each has a constant latitude increment of 2.5°. Considering only the northern hemisphere, at the equatorial latitude zone (0° to +2.5° latitude zone 37) a longitude box of 2.5° is used. Thus there are 144 equal area boxes in this latitude zone. The area computed from here is then used to find the appropriate longitude increment of the equal area boxes in all other latitude zones. By the pole there are only 3 equal area boxes with a base longitude of 120°.

The computer programs supplied with the ISCCP C2 data tapes unpack the data from binary format and remap it onto a 2.5° equal angle grid. This is done by the simple replication of data from the equal area grid to the appropriate equal angle grid. As a first approximation it appears reasonable to manipulate the ISCCP data from the 2.5° equal angle grid results provided.

Consider the case where the AGCM results to be validated by ISCCP have a different longitudinal resolution to 2.5°. For example the UK Meterological Office 11 layer model has a resolution of 2.5° in latitude but 3.75° in longitude. Each ISCCP equal angle grid square can be considered to be composed of a number of pixels n of which r have been defined as cloudy. In area-weighting a subset m of the pixels of which s are cloudy will be used. If the r cloudy pixels are spatially independent and randomly

distributed in the grid square, then the distribution of s can be described by the hypergeometric function.

$$P_s(s) = \frac{{}^{r}C_s \; {}^{n-r}C_{m-s}}{{}^{n}C_m}$$

the mean of which is given by

$$E(s) = \frac{mr}{n}$$

the variance is given by

$$Var(s) = \frac{m \; r \; (n-r) \; (n-m)}{n \quad n \quad (n-1)}$$

The accuracy with which the cloud amount will be transferred is dependent upon the proportion of the grid square used in the weighting as well as the number n of cloudy pixels. The greatest inaccuracy occurs when 50% of the pixels are cloudy and 50% grid square area is weighted. As accuracy is dependent on the proportion of the grid square weighted, certain latitude zones will be more accurate than others, where the model grid square is some exact multiple of the equal angle longitude increment.

The replication used by ISCCP is a crude form of area weighting. Table 2 shows the differences between the zonal mean total cloud amount calculated from the equal area grid and the equal angle

grid for January 1984, 20° north to south. The difference between them is caused by the replication procedure, though, as can be seen, the difference is small.

For validation of model output Rossow and Garder (1984) suggest using the equal area ISCCP data in comparing ISCCP data to model output. Model output is invariably equal angle in its spatial distribution. Therefore some area-weighting is inevitable. The errors induced may be further complicated in that it is unlikely that cloud covered pixels are randomly distributed, except in broken cloud fields, more likely is a clumped distribution.

In the results presented in the following sections zonal means are calculated from the equal area grid as recommended by Rossow and Garder (1984). However for ease of graphical presentation the global data is presented on the equal angle grid.

Zonal Means

As explained earlier the ISCCP C2 data set is arranged into 72 latitude zones, each zone is 2.5° in latitude. Using data from the equal area grid the zonal mean for each of the 72 latitude zones was calculated. The results were calculated for the two extreme seasons, using data from December 1983, January and February 1984, and, June, July, and August 1984. From herein these will be referred to as DJF and JJA respectively.

(a) Seasonal Zonal Means for 1984

Figures 2(a) and (b) show the zonal total cloud amount, and low, middle and high cloud frequency of occurrence as retrieved by ISCCP for the two seasons DJF and JJA respectively. The ISCCP zonal total cloudiness agrees well with the traditional surface cloud climatologies, see for example London (1957), Van Loon (1972) and Hughes (1984). All the familiar features are present. The equatorial maximum occurs at 10°N during the JJA period which corresponds to the position of the Intertropical Convergence Zone (ITCZ) at this time. The double equatorial maxima (5°N and 10°S) present in the DJF chart (Figure 2(a)) are detectable in other zonal cloud climatologies notably Clapp (1964), Sadler (1969) and Schutz and Gates (1971) as derived by Hughes (1984). These are all based on satellite retrieved cloudiness (Schutz and Gates (1971) include some surface-based observations). The ITCZ migrates southwards during the northern hemisphere winter. This migration is small over the oceans but large over the continents. Traditional cloud climatologies based on surface observations will have little input from ocean areas. Consequently a single equatorial maximum in cloud amount, associated with the large southerly movement of the ITCZ over the continents, will be observed. The more uniform spatial coverage afforded by satellites and the consequent increased input from over the oceans result in satellite cloud climatologies recording double maxima, the more northerly maximum being associated with the position of the ITCZ over the ocean. The sub-tropical minima occur in both DJF and JJA, located around 15° in the winter

hemisphere and 25° in the summer hemisphere, although the summer hemisphere minima are smaller, particularly in the southern hemisphere. There is a mid-latitude maximum, 55° in the summer hemisphere and 50° in the winter hemisphere. This maximum is greatest in the southern hemisphere. This is most likely due to the greater land mass in the northern hemisphere and the large areas of clear skies associated with these areas. This is difficult to confirm from these zonal means alone and is discussed again in the next section. The most significant disagreement between the ISCCP climatology and previous climatologies comes at the polar regions. The large polar cloudiness in the summer hemisphere, indicated in previous cloud climatologies, is not observed. In the southern hemisphere there is a marked minimum with total cloud amounts of less than 10%. Indeed for both poles the maximum cloudiness occurs in the winter hemisphere. This could be due to various factors. Firstly, the ISCCP zonal cloud climatology presented is based on only one year of data and there could be great interannual variability. Secondly, due to the similarity of snow/ice reflectance and brightness temperatures to clouds, satellite retrievals have difficulty retrieving cloud cover over snow/ice, the cloud cover retrieved could be in error. A third explanation is the previous lack of cloud observations in the polar interior. Schwerdtfeger (1984) notes that in Antarctica the variation of cloud cover with latitude is most noticeable. With a greater frequency of cloudy skies occurring in both summer and winter at the lower latitudes, over the southern oceans and along the coasts, than at high latitudes, over the ice sheet. For example Faraday at 65.3°S has

cloudy skies 82% of the time in winter and 77% of the time in Summer, whereas South Pole 90°S has cloudy skies 18% of the time in winter and 11% in summer. The surface observations from Warren et al. (1986) indicate a minimum in total cloud amount at the South Pole, the amount rising quickly towards the coast. However the minimum is greatest during winter (JJA) and the values similar to that of Berlyand and Strokina (1980). Attributing any one of these factors as the reason for the difference between the ISCCP polar cloudiness and previous climatologies is difficult and it is likely that all contribute to some extent.

By looking at the frequency of occurrence of the different cloud types ISCCP provides an opportunity to examine the vertical make up of the distribution of total cloudiness. Immediately noticeable is that the southern hemisphere mid-latitude maximum is frequently composed of low cloud with middle clouds making a significant contribution at the higher latitudes. During daylight hours the ISCCP cloud levels are further subdivided into cloud types. Examination of the daylight cloud types (Figure 3, 4 and 5) implies that in the tropics stratus and cumulus (Figure 3) occur with about the same frequency. However the stratus reaches a distinct maxima at mid-latitudes in the southern hemisphere summer (Figure 3(a)). A maximum of stratus occurrence can also be seen in the northern hemisphere summer (JJA) when looking at ocean only grid squares (not shown). This agrees well with Warren et al. (1988) where the most frequently occurring cloud type at mid-latitudes is Stratus. For middle level clouds (Figure 4) at latitudes higher than 40° north and south, nimbostratus occurs

more frequently than alto-cumulus. In DJF (Figure 4(a)) there are distinct maxima of nimbostratus occurrence corresponding with the mid-latitude depression systems. In JJA (Figure 4(b)) the maximum is still evident although weaker in the northern hemisphere. This is again in good agreement with that found by Warren et al. (1988).

The sub-tropical minima appear to be a region of minimum occurrence of high and middle cloud, particularly the winter hemisphere sub-tropical minima. The near equatorial maximum coincides with a maximum in high level cloud frequency (Figure 5). This is not surprising given the deep convective activity that occurs in this region. The daylight cloud types show a maxima of deep convective, cirrostratus and cirrus here. Noticeable also is the maximum in middle level cloud occurrence (Figure 4) which from daylight cloud types is predominantly alto-cumulus, which again, given the activity of the region, might be expected.

Care must be taken in interpreting these results. As was pointed out in the introduction satellite retrievals contain basic problems and limitations. The most influential for layer clouds is that high cloud will obscure lower cloud from the satellite sensor's view (Sèze et al., 1987). Over Antarctica in JJA the total cloud amount is almost entirely composed of high cloud. However this is likely to be a true appraisal of the vertical distribution of cloud cover. Surface observations of clouds record that low clouds such as stratus rarely occur at any time

during the year (Schwerdtfeger, 1984). The small amount of snowfall on the high plateau in Antarctica confirm such observations. Cumuliform clouds are very occasionally seen in summer. In contrast high cloud at the near equatorial maximum will undoubtedly hide low cloud. It is difficult to say whether the apparent minimum of low cloud at 10°N in JJA is a real minimum or due to high and middle level cloud obscuring the low cloud. Warren et al. (1988) certainly indicate the greater presence of cumulus over the oceans. The lack of high and middle level cloud in the summer sub-tropical minima will mean a more accurate appraisal of the low cloud amount.

It could be tentatively argued given this limitation, that although low cloudiness is more frequent in the southern hemisphere it is far more uniform that might be first concluded. The greatest variability is found in high and middle cloud occurrence.

(b) Zonal Means over Oceans Only

Zonal means were calculated for those ISCCP grid squares that were classified as Ocean only and are shown in Figure 6. The overall shape of the total cloudiness distribution remains similar but immediately apparent is the increased mid-latitude maximum in the northern hemisphere in both extreme seasons. This confirms the assertion in the previous section of the effect of the greater land mass area in the northern hemisphere on cloudiness. From comparing Figures 2 and 6 the greatest

contribution to this increase comes from a greater occurrence of low clouds over the oceans. In the DJF (Figure 6(a)) period the maximum in total cloud amount at 5°N takes on increased importance, with the maximum at 10°S almost lost. The maximum in high cloud occurrence at this latitude is reduced from that shown in Figure 2(a). This is as expected, the maximum at 10°S, being due to the position of the ITCZ over land. The total cloud amount (Figure 6) for the most part agrees well with Warren et al. (1988). The areas of significant difference again occur at the polar regions. During DJF (Figure 6(a)) Warren et al. (1988) record a much smaller total cloud amount at latitudes greater than 70°N. At 90°N ISCCP implies a total cloud amount of 70% whereas Warren et al. (1988) find less than 50%. During JJA the opposite is true with Warren et al. (1988) recording greater than 80% total cloud cover and ISCCP observing less than 50% for 1984 over the arctic. Again the differences could be due to interannual variability, poor satellite cloud retrieval over snow and ice, or lack of surface observers. The distribution of middle and high cloud frequency of occurrence remains remarkably similar to that shown in Figures 2(a) and 2(b). The main difference occurring at high latitudes during JJA (Figure 6(b) when high cloud frequency is greatly increased.

Zonal Mean Cloud Water Path

In Figure 7(a) and 7(b) the cloud water path in gm^{-2} is shown for DJF and JJA respectively. There is an extremely uniform appearance at the lower latitudes, with little change from one

latitude zone to the next. A small maximum coincides with the near equatorial maximum of total cloudiness at 5-10°N in both extreme seasons. The total water path moves quickly to a small minima, then rises steadily with increasing latitude to a spectacular increase with high latitudes. This rapid increase does not correspond with the mid-latitude maximum in total cloudiness, occurring as it does at higher latitudes. The increase is not so large in the summer hemisphere.

In order to compare these results with those by Smith (1990) the zonal mean cloud water path over the oceans were calculated. The results are shown in Figure 8. It should be stressed that the values from ISCCP C2 data are based on a linear average of the cloud optical thickness values and is a total cloud water path. The values in Smith (1990) are for liquid water path only. It can be seen in Figure 8 that at low latitudes the ISCCP data is far more uniform that either that predicted by the United Kingdom Meteorological Office 11 layer model or from the SMMR data of Njoku and Swanson (1983). The northern hemisphere is in reasonable agreement with the satellite data, but the southern hemisphere is far lower at the mid-latitudes. The only area of any reasonable agreement between the model results and ISCCP is at low latitudes.

Given that ISCCP is total water path and the other results discussed are for liquid water path only, the low values of ISCCP are surprising. It is now known (Rossow, p.c., 1991) that the current values of PATH are too low, by about 30%, due to improper

averaging over the spatial domain. Allowing for this would certainly improve the results, however the southern hemisphere ISCCP values would still be significantly lower than those shown in Smith (1990). The large cloud water path reported by ISCCP at high and polar latitudes will be discussed in more detail later.

Global Maps

Again data for the two extreme seasons DJF and JJA are presented. For ease of presentation the equal angle grid is used (2.5° by 2.5°). The coastlines are those indicated by the surface type codes in ISCCP.

(a) Cloud Cover

The full global maps of total cloud amount are presented in Figure 9. Although the climatology is only for the year of 1984 it appears to agree well with previously published cloud climatologies (London, 1957, Berlyand and Strokina, 1980, Hughes, 1984, and Hughes and Henderson-Sellers, 1985). With the following points:

(i) During DJF (Figure 9(a)) both the northern and southern hemisphere oceans exhibit a cloud amount maximum, greater than 90% over large areas, associated with the mid-latitude depression systems. In the southern hemisphere, during JJA, areas exhibiting

greater than 90% cloud cover contract. This agrees with Berlyand and Strokina (1980).

(ii) There is a cloud amount minimum in the oceanic regions associated with the subtropical high pressure systems.

(iii) There is a continental cloud amount minimum associated with all the Earth's desert regions.

(iv) The Southern Asian monsoon is clearly visible in the increase of cloud cover over the region from the DJF to the JJA charts. The increase appears reasonable in comparison to Berlyand and Strokina (1980) and Warren et al. (1986 and 1988).

(v) There is an equatorial maximum of cloud cover associated with the position of the ITCZ.

(vi) During DJF the Arctic is an area of cloud maximum whereas the Antarctic an area of cloud minimum. In JJA Antarctica is still an area of relatively small cloud amounts. This corresponds well with the surface based results (Schwerdtfeger, 1984).

From global plots of the frequency of occurrence of the three cloud types, low, middle and high (Figures 10, 11 and 12), more can be said about the cloud distribution. Low cloud occurs for 30% of the time over most of the oceans (Figure 10). In contrast the interior of continents, especially in the winter hemisphere are devoid of low cloud most of the time. Low cloud occurs with a frequency of 10% or less. How much of this is a feature of the downward looking satellite sensor rather than a real lack of low level cloud is difficult to assess and will vary geographically. Surface observations from Warren et al. (1986) suggest a much greater frequency of occurrence of low cloud, apart from over the worlds desert regions and north east USSR, where low cloud does occur less frequently. In Figure 10 during both extreme seasons (DJF and JJA) areas of low cloud maximum (occurring at least 50% of the time) can be seen at sub-tropical latitudes to the west coasts of the continents. These areas agree well with the position of marine stratocumulus shown by Hanson (1991). The areas have a maximum coverage during DJF (Figure 10(a)), the northern hemisphere summer, which corresponds well with the known maximum areal extent of marine stratocumulus.

Particularly noticeable in Figures 11 and 12 are large areas where the frequency of occurrence of high and middle level cloud is 10% or less. These cover the Afro-Asian dessert and areas either side of the near equatorial maximum over the oceans extending to the sub-tropics. These oceanic areas correspond well with the Trade Wind area. The inversion layer which exists across

the Trade Winds prevents the upward movement of air and the formation of cloud is limited to the lower Trade Wind layer.

The position of the near equatorial maximum is easily visible in the large values of high cloud frequency in DJF (Figure 12(a)). With values of 50% over Southern Africa and Indonesia. The distribution agrees well with the distribution of daylight frequency of occurrence of cirro cloud types from Warren et al. (1986). Mid-latitude cyclonic activity can also be detected. In the JJA period (Figure 12(b)) the Monsoon is an area with high cloud occurring up to 70% of the time. Again this distribution agrees well with Warren et al. (1986).

(b) Cloud Water Path

The cloud water path plots can be seen in Figure 13. As might be expected the water path between 45°N and 45°S shows a similar distribution to the cloud amount. Up to 70°N in JJA and 70°S in DJF the agreement is reasonable. However at higher latitudes there appears to be a large discrepancy between the cloud amount and the water path. With an extremely large cloud water paths being recorded.

Different cloud types will obviously effect the cloud water path and this may well be a factor. However the rise is so dramatic and appears confined to the high polar latitudes and might be due to the difficulty of retrieving cloud parameters over snow and ice. The ISCCP C2 data contains a variable for snow/ice amount

which was plotted (not shown) to see if the regions coincided. Many areas of large cloud water path occurred over areas which are almost 80 to 100% covered by snow or ice. Indeed Rossow (p.c. 1991) confirms that the polar optical thicknesses from which PATH is derived are far too high as the retrieval over bright surfaces has two solutions and currently the upper solution is being used. This does not explain all the large cloud water path values, for example over east Asia USSR in DJF. The assumption of a constant cloud particle size distribution might well be in error. However it ought to be pointed out that Walker and Rossow (1991) refer to PATH as an *estimate* of the cloud water path. Kriebel et al. (1989) put an uncertainty estimate on their cloud water paths determined by the APOLLO system as ± 50%.

Discussion

The small number of parameters discussed in this paper represent a minute fraction of the data available through ISCCP. With such a vast new resource it will take time to discover its full potential. Unfortunately its size may well limit its use to those within the large climate modelling groups who have the resources to tackle such data volumes. It may, therefore, seem unreasonable, to request more parameters. However water content and mean of cloud amount when present, for the three cloud types low, middle and high would be very useful. As climate modellers seek to include cloud optical properties in climate models, water path for the individual cloud types would provide a useful validation tool. Also as Slingo (1991) reports much effort is

being centred on predicting "surface observed" cloud and radiances from satellite data. The information on layer cloud amount in conjunction with the work of Warren et al. (1986 and 1988) would provide a valuable resource for such an undertaking.

The zonal means and full globe maps of total cloud amount agree well with previous cloud climatologies. This climatology has been based on one year only. Several more years of C2 data have become available since the writing of this paper. To use a satellite global cloud climatology in conjunction with surface observed data such as Warren et al. (1986 and 1988), may require at least a decade of satellite data. Warren et al. (1986 and 1988) currently provide one of the few data sources on surface based global layer cloudiness. It is also available digitally which should allow a comprehensive quantitative analysis of these in conjunction with ISCCP.

ISCCP provides some of the first global views of cloud optical properties, such as cloud water path. It is these properties which decide the cloud effect on the radiation budget which is the real goal of climate modellers. From the results and comments above, obviously more work is required on retrieving these properties, but the very nature of the ISCCP data sets allows this to occur. It is important that such work should be encouraged and the results widely disseminated.

Acknowledgements

I would like to thank John Lockwood for his comments and encouragement. I would also like to thank William Rossow for answering questions about the ISCCP C2 data and John Byrne for helping with the statistics.

References

Berlyand, T.G. and Strokina, L.A. 1980, *'Global distribution of total cloud amount'*, Leningrad, Gidromteoizdat, (translated by S. Warren). p. 71.

Buriez J.-C., Bonnel, B., Fouquart, Y., Geleyn, J.-F. and Morcrette, J.-J. 1989. 'Comparison of model-generated and satellite-derived cloud cover and radiation budget', *J. Geophy. Res.*, ***93***, 3705-3719.

Drake, F. 1987. *'Exploiting surface observations of cloudiness for global-scale nephanalyses'*, Unpublished Ph.D. Theses, University of Liverpool. p. 450.

Clapp, P. F., 1964, 'Global cloud cover for seasons using TIROS nephanalyses', *Mon. Wea. Rev.*, **92**, 495-507.

GARP, 1978. *'JOC Study Conference on Parameterisations of Extended Cloudiness and Radiation for Climate Models'*, Oxford, England. GARP Climate Dynamics Subprogram. World Meterological Organisation, Geneva.

Hanson, H.P. 1991. 'Marine stratocumulus climatologies', *Int. J. Climatol.*, **11**, 147-164.

Houghton, J.T., Jenkins, G.J. and Ephraums, J.J. 1990. *'Climate Change, The IPCC Scientific Assessment'*, Cambridge University Press, Cambridge. p. 365.

Hughes, N.A. 1984. 'Global cloud climatologies: An historical review', *J. Clim. Appl. Meteor.*, **23**, 724-751.

Hughes, N.A. and Henderson-Sellers, A. 1985. 'Global 3D-Nephanalysis of total cloud amount: Climatology for 1979', *J. Clim. Appl. Meteor.*, **24**, 669-686.

Kriebel, K.T., Saunders, R.W. and Gessell, G. 1989. 'Optical properties of clouds derived from fully cloudy AVHRR pixels', *Contrib. Atmos. Phys.*, **62**, 165-171.

London J. 1957. *'A study of atmospheric heat balance. Final Report'*, AFCRC-TR-57-287, New York University.

Malberg, H. 1973. 'Comparison of mean cloud cover obtained by satellite photographs and ground based observations over Europe and the Atlantic, *Mon. Wea. Rev.*, **101**, 893-897.

Morcrette J.-J. 1991. 'Validation of model-generated cloudiness: satellite -observed and model-generated diurnal variability of brightness temperature', Accepted for publication in *Mon. Wea. Rev.*

Njoku, E.G. and Swanson, L. 1983. 'Global measurements of sea surface temperature, wind speed and atmospheric water content from satellite microwave radiometry', *Mon. Wea. Rev.*, **111**, 1977-1987.

Rossow, W.B. 1989. 'Measuring cloud properties from space: A review', *J. Climate*, **2**, 201-213.

Rossow, W.B. and Garder, L. 1984. 'Selection of a map grid for data analysis and archival', *J. Clim. Appl. Meteorol.*, **23**, 1253-1257.

Rossow, W.B., and Schiffer, R.A. 1991. 'ISCCP Cloud Data Products', *Bull. Amer. Met. Soc.*, **72**, 2-20.

Rossow, W.B., and Walker, A.W. 1991. *'Appendix C: International Satellite Cloud Climatology Project (ISCCP) Description of Monthly Mean Cloud Data (Stage C2)'*, WMO/ICSU.

Sadler, J.C. 1969. *'Average Cloudiness in the Tropics from satellite observations, International Indian Ocean Expedition.'* Meteor. Monogr. No. 2, East West Center Press, Honolulu. p. 22.

Schutz, C., and Gates, W.L. 1971. *'Global climatic data for surface 800mb and 400mb: January. A report prepared for Advanced Research Projects Agency'*, Rand, Santa Monica, R-915-ARPA,

Schwerdtfeger, W., 1984. *'Weather and Climate of the Antarctic'*, Developments in Atmospheric Science 15, Elsevier. p. 261.

Sèze, G., Drake, F., Desbois, M., Henderson-Sellers, A. 1987. 'Total and low cloud amounts over France and southern Britain in the summer of 1983: Comparison of surface-observed and satellite retrieved values', *Int. J. Remote Sensing* , **7**, 1031-1050.

Slingo, A. 1989. 'Wetter clouds dampen global greenhouse warming', *Nature*, **341**, 104.

Slingo, A. 1991. Book Review, *Climatic Change*, **18**, 111-112.

Slingo, J.M. 1987. 'The development and verification of a cloud prediction scheme for the ECMWF model', *Q. J. R. Meteorol. Soc.* , **113**, 899-927.

Smith, R.N.B. 1990. 'A scheme for predicting layer clouds and their water content in a general circulation model', *Q. J. R. Meteorol. Soc.*, **116**, 435-460.

Van Loon 1972. *'Cloudiness and precipitation in the Southern Hemisphere'*, Meteorology of the Southern Hemisphere, Meteor. Monogr., No. 13 C.W. Newton. Ed., 101-111.

Warren, S.G., Hahn, C.J., London, J., Chervin, R.M. and Jenne, R.L. 1986. *'Global distribution of total cloud cover and cloud*

type amounts over land', NCAR/TN-273+STR, National Center for Atmospheric Research, Boulder, Colorado. p. 21 + 199 Maps.

Warren, S.G., Hahn, C.J., London, J., Chervin R.M. and Jenne, R.L. 1988. *'Global distribution of total cloud cover and cloud type amounts over the ocean'*, NCAR/TN-317+STR, National Center for Atmospheric Research, Boulder, Colorado. p. 42 + 170 Maps.

Figures

Figure 1. Schematic defining ten radiometric cloud types by the measured values of cloud top pressures and optical thicknesses (from Rossow and Schiffer, 1991, by permission of the American Meteorological Society)

Figure 2. Zonal means for total cloud amount (solid line) and low (dotted line), middle (dash-dot line) and high (dashed line) cloud frequency: (a) for DJF, (b) for JJA.

Figure 3. Zonal means for frequency of occurrence of cloud types (daytime only) for cumulus (solid line) and stratus (dashed line) (a) for DJF (b) for JJA. clouds

Figure 4. As for Figure 3 but for alto-cumulus (solid line) and nimbostratus (dashed line) clouds.

Figure 5. As for Figure 3 but for deep convective (solid line), cirrus (dot-dash line) and cirrostratus (dashed line) clouds.

Figure 6. As for Figure 2 but for ocean only grid squares.

Figure 7. Zonal means for total cloud water path for (a) DJF and (b) JJA.

Figure 8. Zonal means for cloud water path for JJA over ocean only grid squares. ISCCP total cloud water path (solid line),

U.K. Meteorological Office 11 layer Model (dashed line), SMMR data 11 July to 10 August (dash-dot line) and 11 September to 10 October (dotted line) for 1978. The last three are liquid water path only. (After Smith, 1990, by permission of the Royal Meteorological Society).

Figure 9. Total cloud amount in percent: (a) for DJF, (b) for JJA. Contours at 10, 30, 50, 70 and 90%. Areas above 70% are shaded.

Figure 10. Low cloud frequency of occurrence in percent: (a) for DJF, (b) for JJA. Contours at 10, 30, 50, 70 and 90%. Areas above 50% are shaded.

Figure 11. As for Figure 10 but for middle cloud.

Figure 12. As for Figure 10 but for high cloud.

Figure 13. Total cloud water path in gm^{-2}: (a) for DJF, (b) for JJA. Contours at 25, 50, 75, 100, 200, 300 and 400 gm^{-2}. Areas above 100 gm^{-2} are shaded.

Tables

Table 1. ISCCP C2 Data Contents (from Rossow and Schiffer, 1991, by permission of the American Meteorological Society)

Cloud amount information

- Monthly average cloud amount
- Monthly frequency of cloud occurrence
- Monthly average IR-cloud amount
- Monthly average marginal cloud amount

Average total cloud properties

- PC, cloud top pressure
- Average spatial and temporal variations of PC
- TC, cloud top temperature
- Average spatial and temporal variations of TC
- TAU, cloud optical thickness
- Average spatial and temporal variations of TAU
- PATH, cloud water path
- Average spatial and temporal variations of albedo

Average properties (amount, PC, TC, TAU) for cloud types

- Low cloud (IR-only)
- Middle cloud (IR-only)
- High cloud (IR-only)
- Cumulus cloud
- Stratus cloud
- Alto-cumulus, alto-stratus cloud

Nimbostratus

Cirrus cloud

Cirro cumulus, cirro-stratus cloud

Deep convective cloud

Average surface properties

TS, surface temperature

Average temporal variations of TS

RS, surface visible reflectance

Snow/ice cover fraction

Average atmospheric properties

PS, surface pressure

TS, surface temperature

T5, temperature at 500mb

PT, tropopause pressure

TT, tropopause temperature

ST, stratospheric temperature

PW, column water amount

O3, column ozone amount

Table 2. Differences between zonal means of total cloud amount based on the equal area and equal angle grid for January 1984.

Latitude	Percentage difference
18.75	0.352
16.25	0.205
13.75	-0.087
11.25	-0.404
8.75	0.062
6.25	0.0
3.75	0.0
1.25	0.0
-1.25	0.0
-3.75	0.0
-6.25	-0.07
-8.75	-0.04
-11.25	-0.125
-13.75	-0.599
-16.25	-0.129
-18.75	0.061

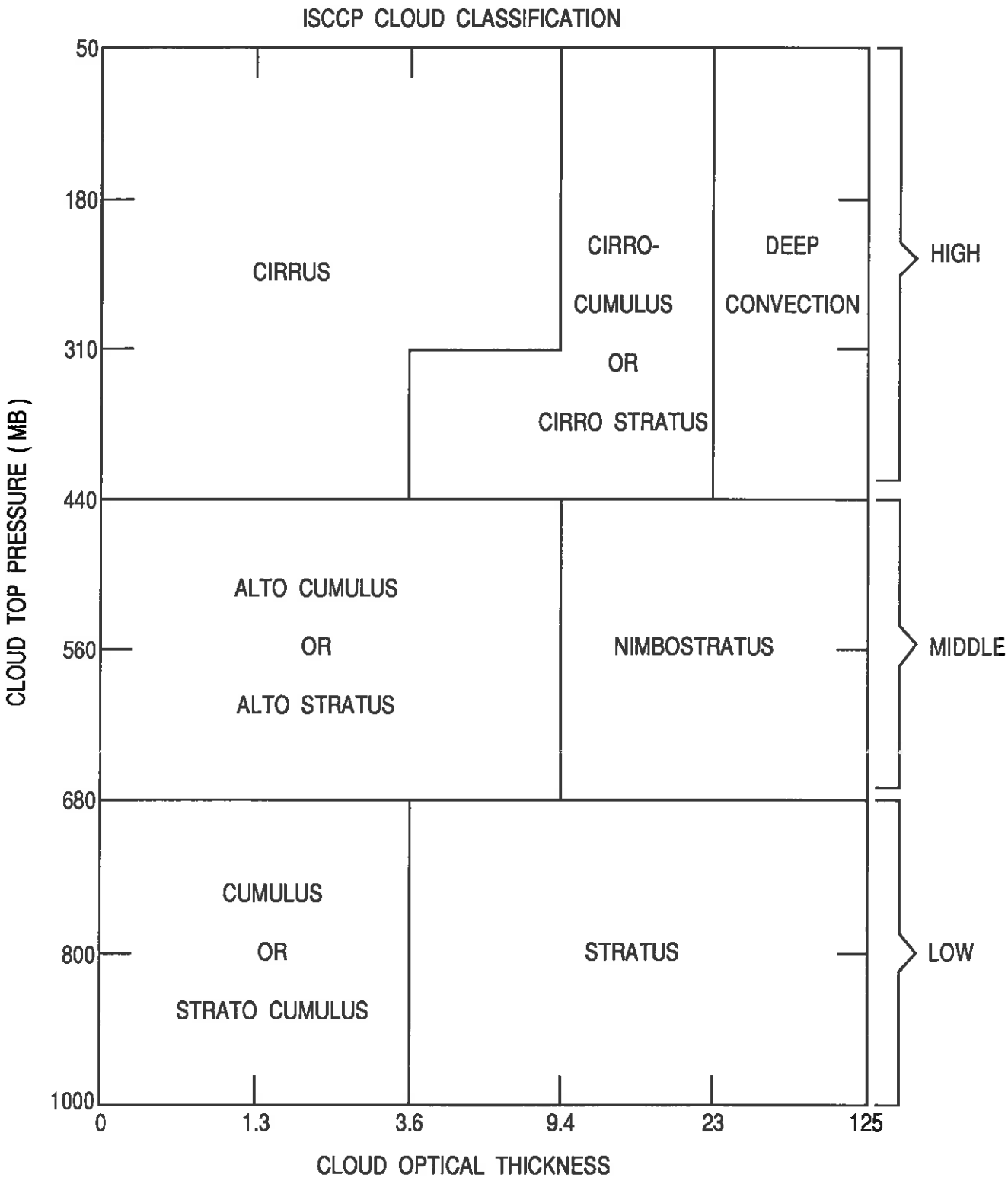
ISCCP CLOUD CLASSIFICATION
CLOUD TOP PRESSURE (MB)
50
180
310
440
560
680
800
1000
CIRRUS
CIRRO-
CUMULUS
OR
CIRRO STRATUS
DEEP
CONVECTION
HIGH
ALTO CUMULUS
OR
ALTO STRATUS
NIMBOSTRATUS
MIDDLE
CUMULUS
OR
STRATO CUMULUS
STRATUS
LOW
0
1.3
3.6
9.4
23
125
CLOUD OPTICAL THICKNESS

Figure 1

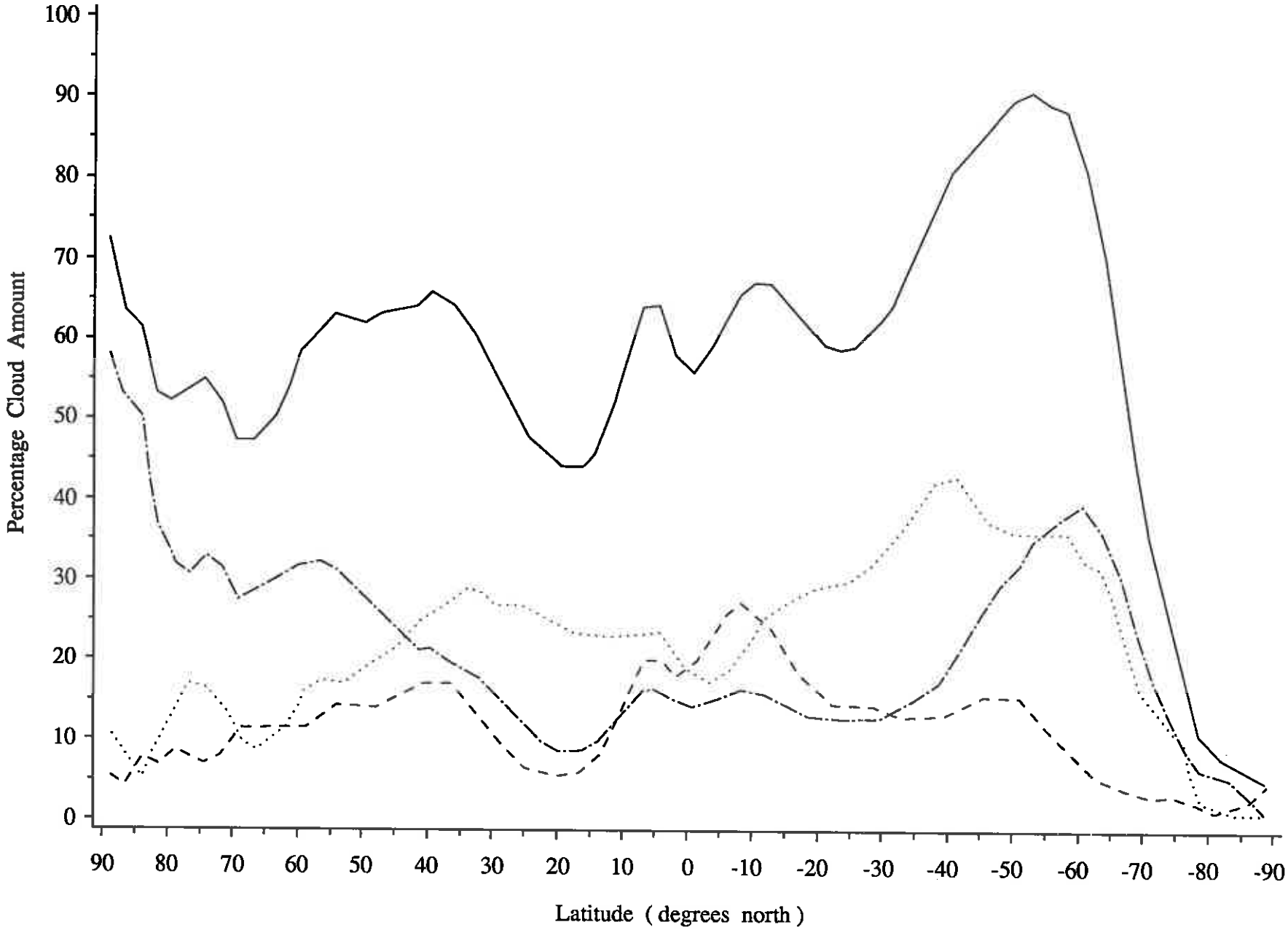
Percentage Cloud Amount
100
90
80
70
60
50
40
30
20
10
0
90 80 70 60 50 40 30 20 10 0 -10 -20 -30 -40 -50 -60 -70 -80 -90
Latitude (degrees north)

Figure 2(a)

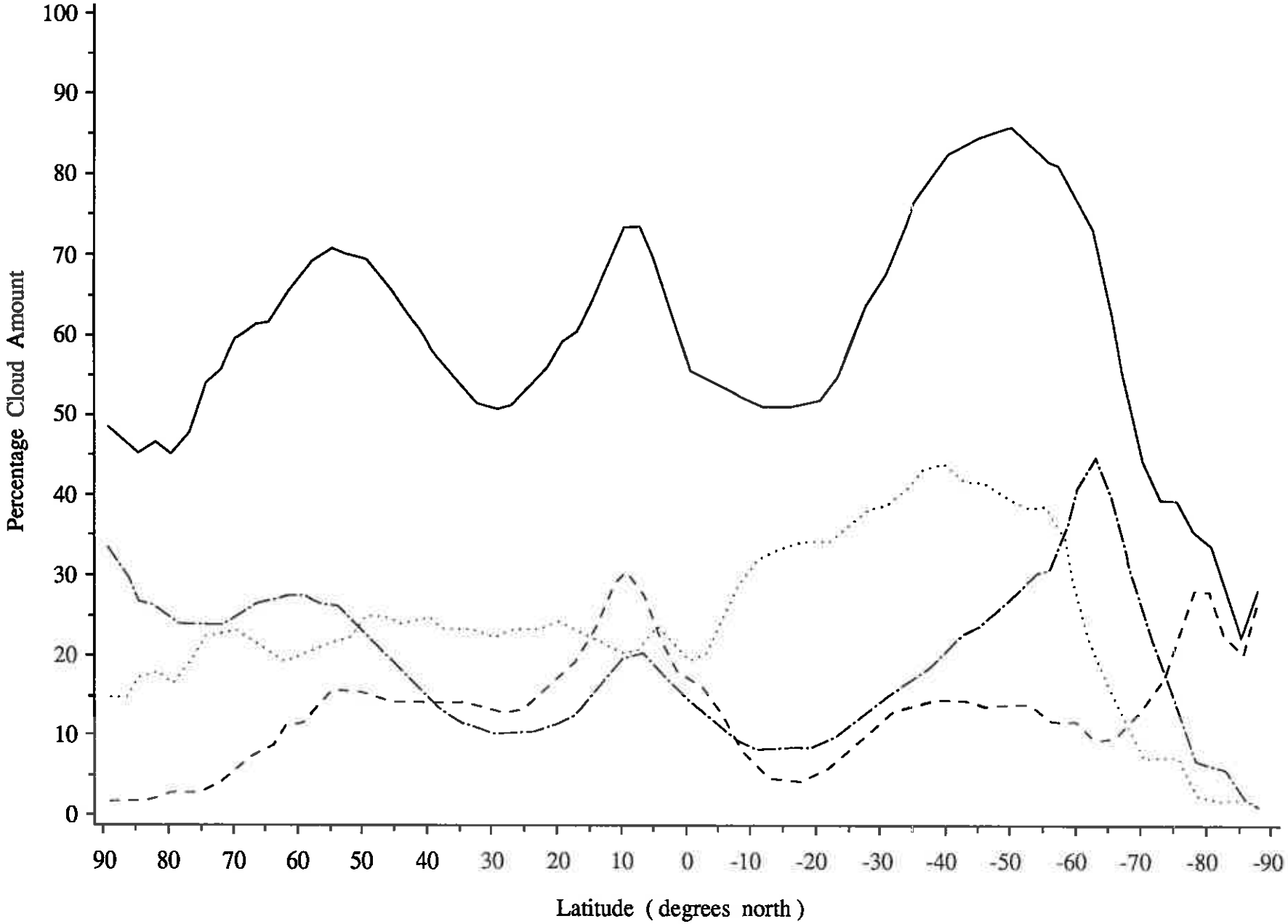
Percentage Cloud Amount
100
90
80
70
60
50
40
30
20
10
0
90 80 70 60 50 40 30 20 10 0 -10 -20 -30 -40 -50 -60 -70 -80 -90
Latitude (degrees north)

Figure 2(b)

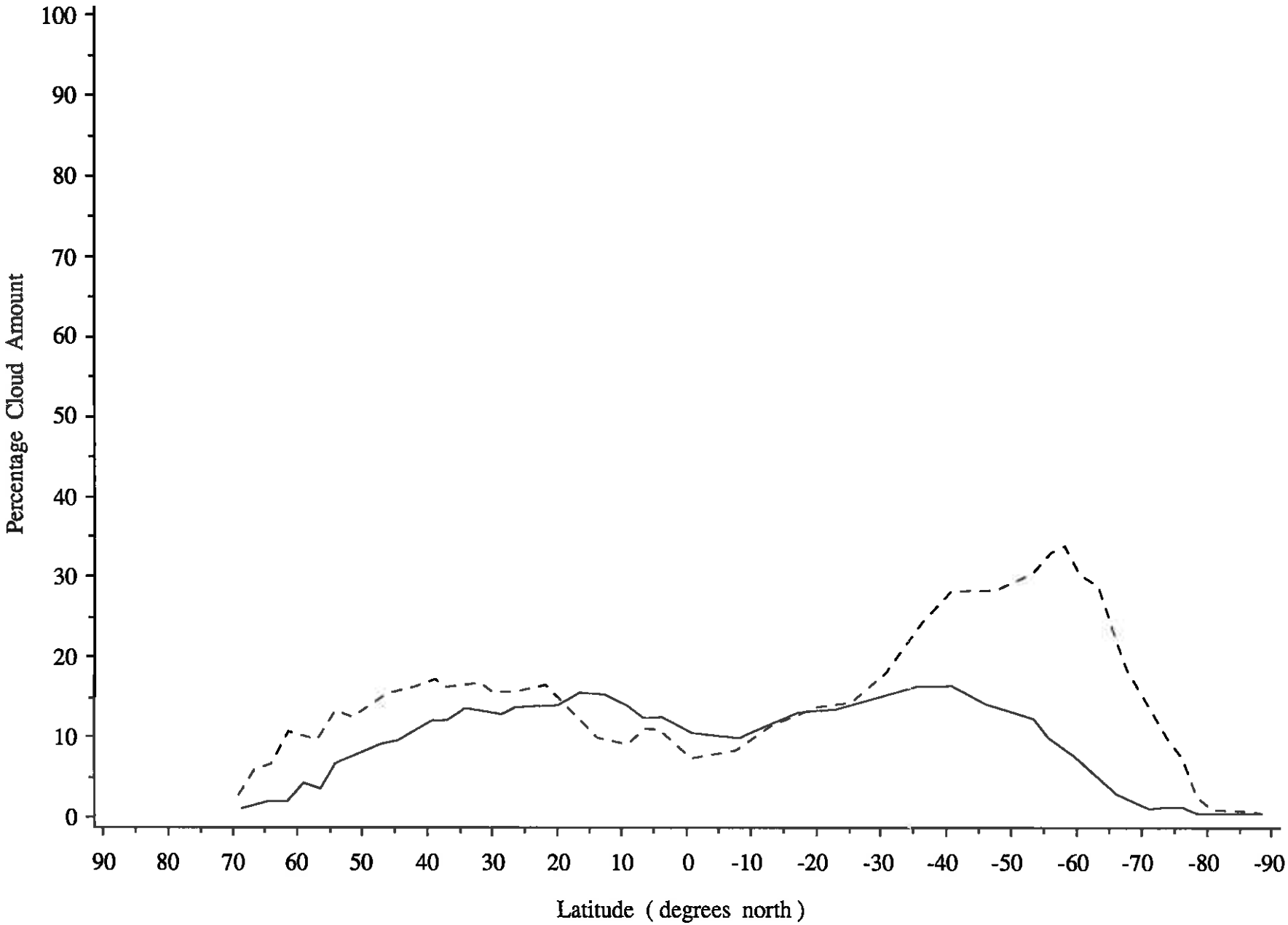
Percentage Cloud Amount
100
90
80
70
60
50
40
30
20
10
0
90 80 70 60 50 40 30 20 10 0 -10 -20 -30 -40 -50 -60 -70 -80 -90
Latitude (degrees north)

Figure 3(a)

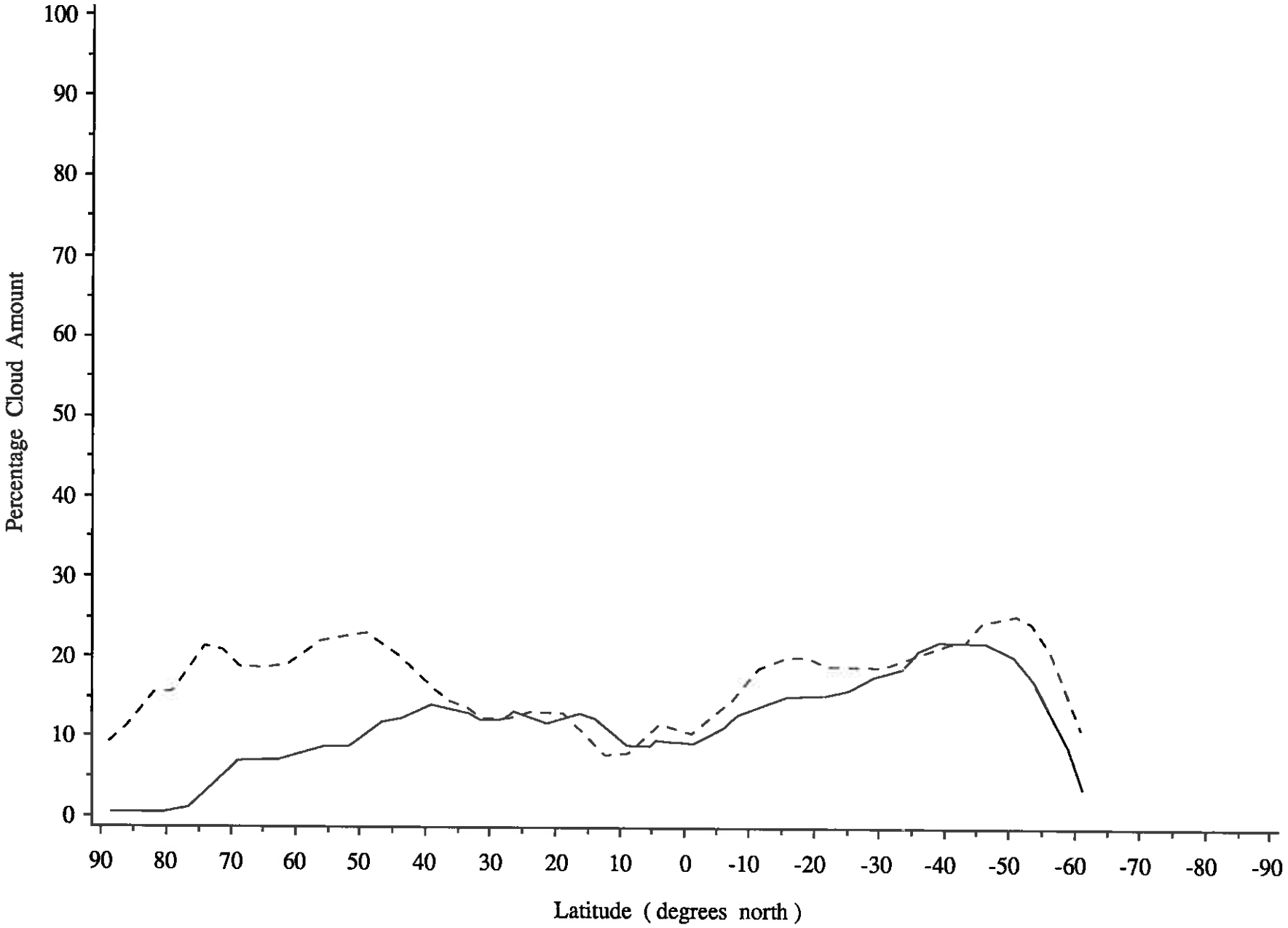
Percentage Cloud Amount
100
90
80
70
60
50
40
30
20
10
0
90 80 70 60 50 40 30 20 10 0 -10 -20 -30 -40 -50 -60 -70 -80 -90
Latitude (degrees north)

Figure 3(b)

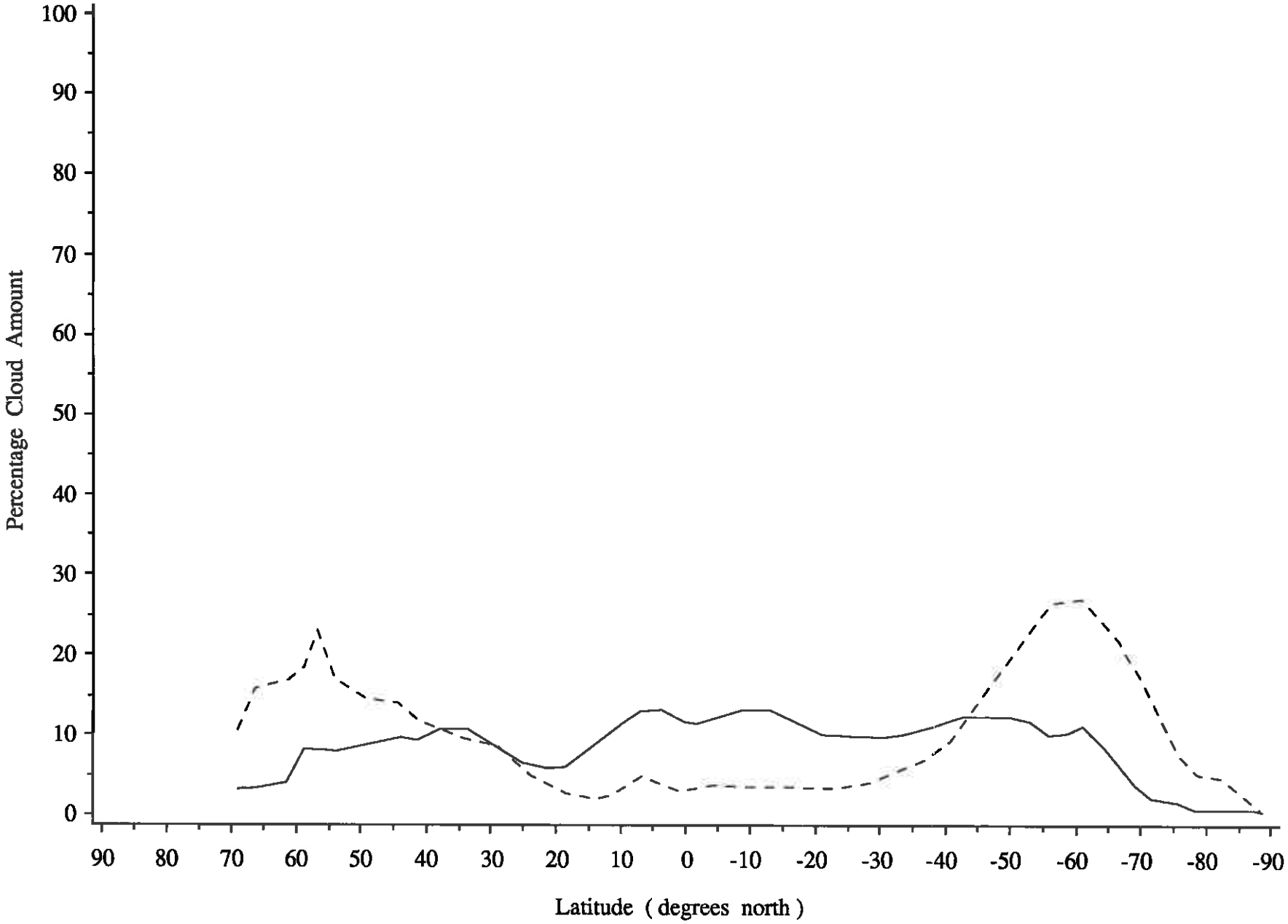
Percentage Cloud Amount
100
90
80
70
60
50
40
30
20
10
0
90 80 70 60 50 40 30 20 10 0 -10 -20 -30 -40 -50 -60 -70 -80 -90
Latitude (degrees north)

Figure 4(a)

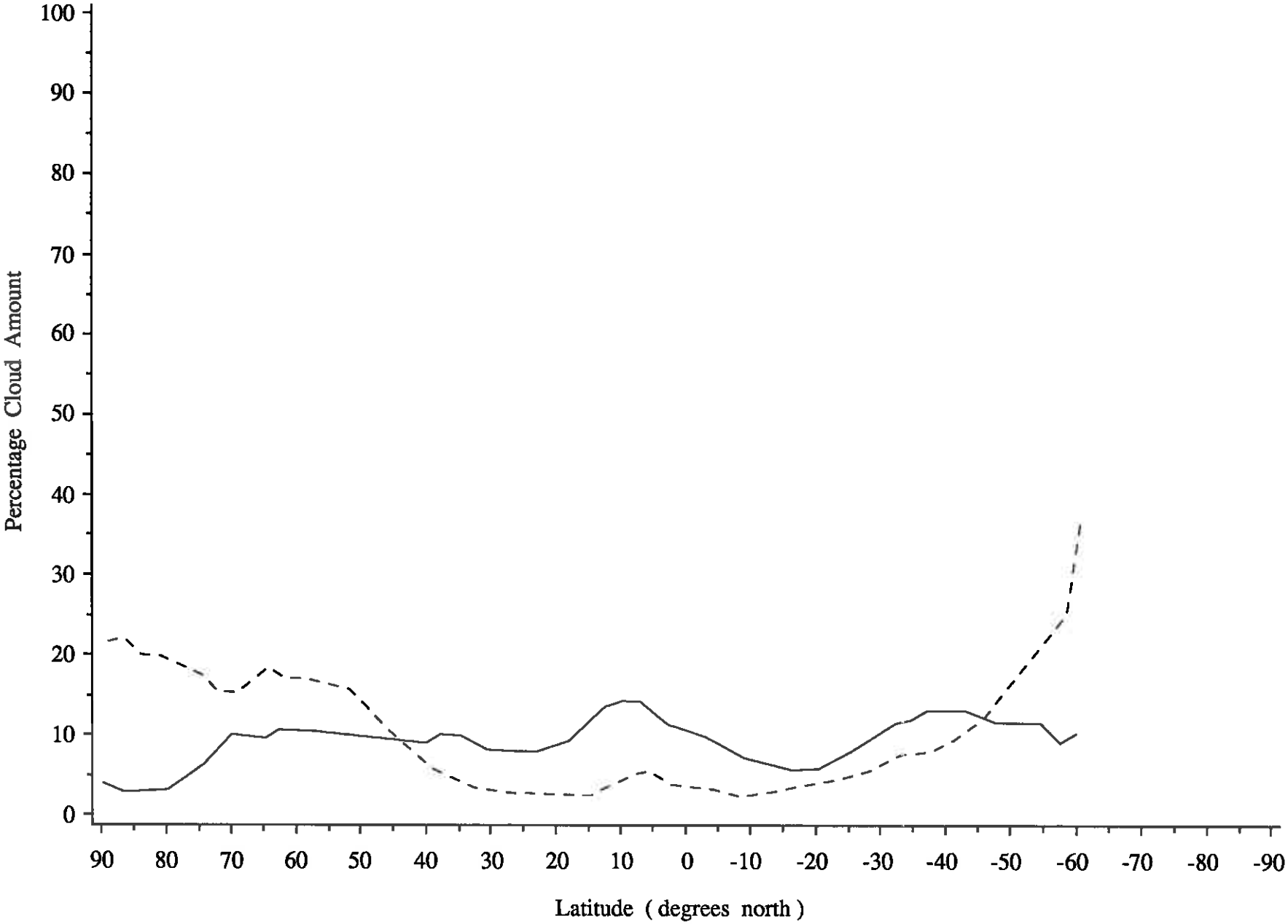
Percentage Cloud Amount
100
90
80
70
60
50
40
30
20
10
0
90 80 70 60 50 40 30 20 10 0 -10 -20 -30 -40 -50 -60 -70 -80 -90
Latitude (degrees north)

Figure 4(b)

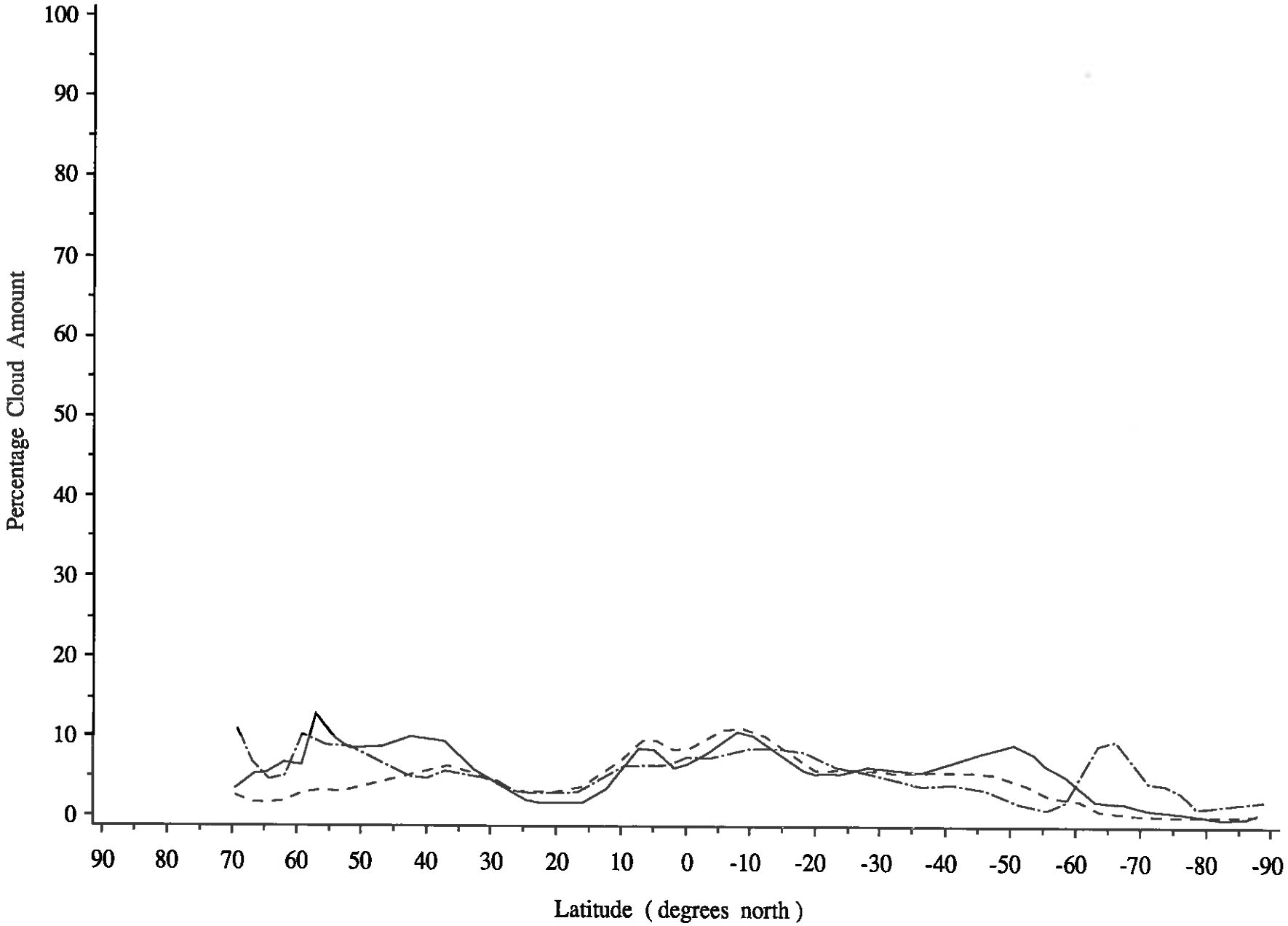
Percentage Cloud Amount
100
90
80
70
60
50
40
30
20
10
0
90 80 70 60 50 40 30 20 10 0 -10 -20 -30 -40 -50 -60 -70 -80 -90
Latitude (degrees north)

Figure 5(a)

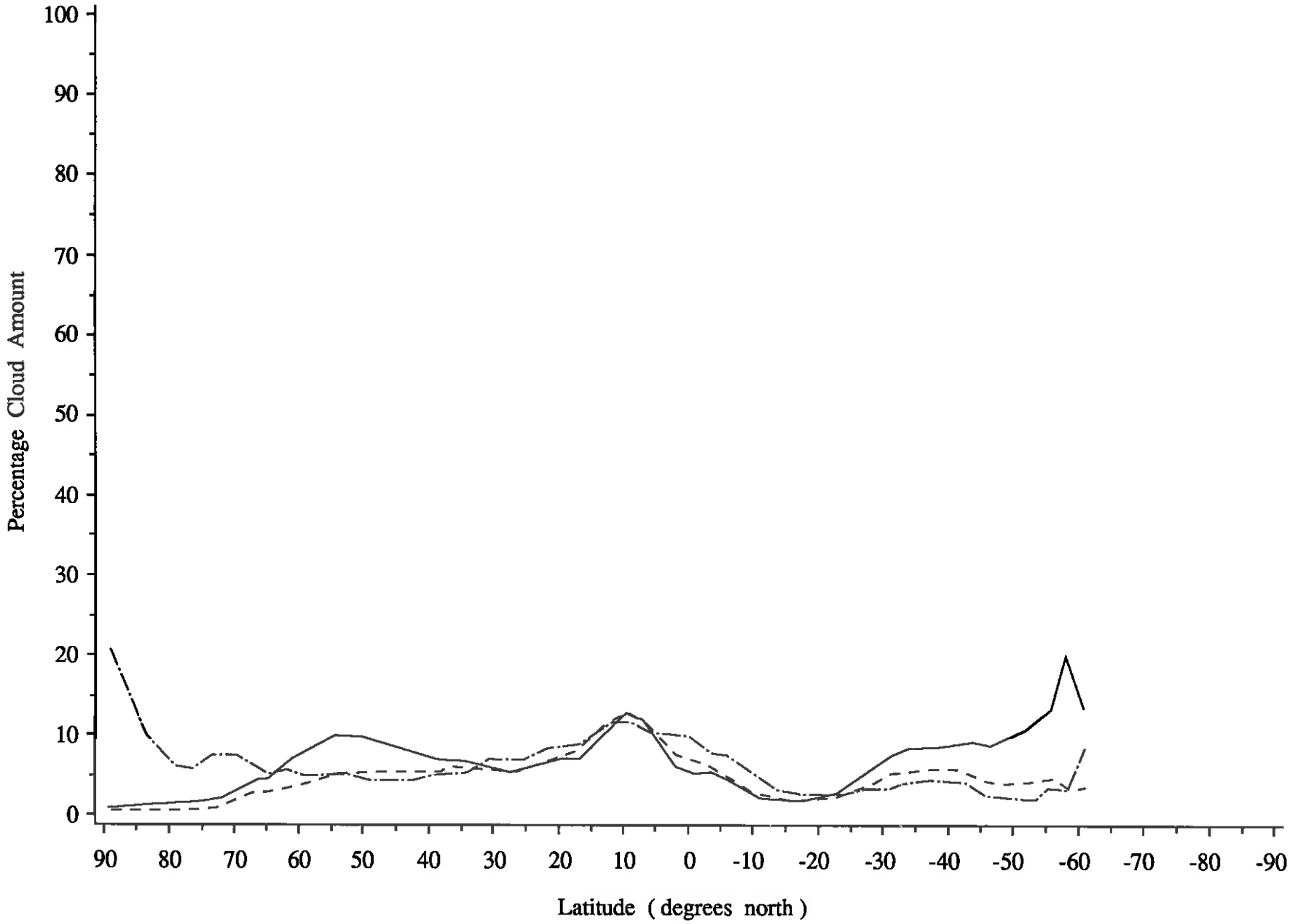
Percentage Cloud Amount
100
90
80
70
60
50
40
30
20
10
0
90 80 70 60 50 40 30 20 10 0 -10 -20 -30 -40 -50 -60 -70 -80 -90
Latitude (degrees north)

Figure 5(b)

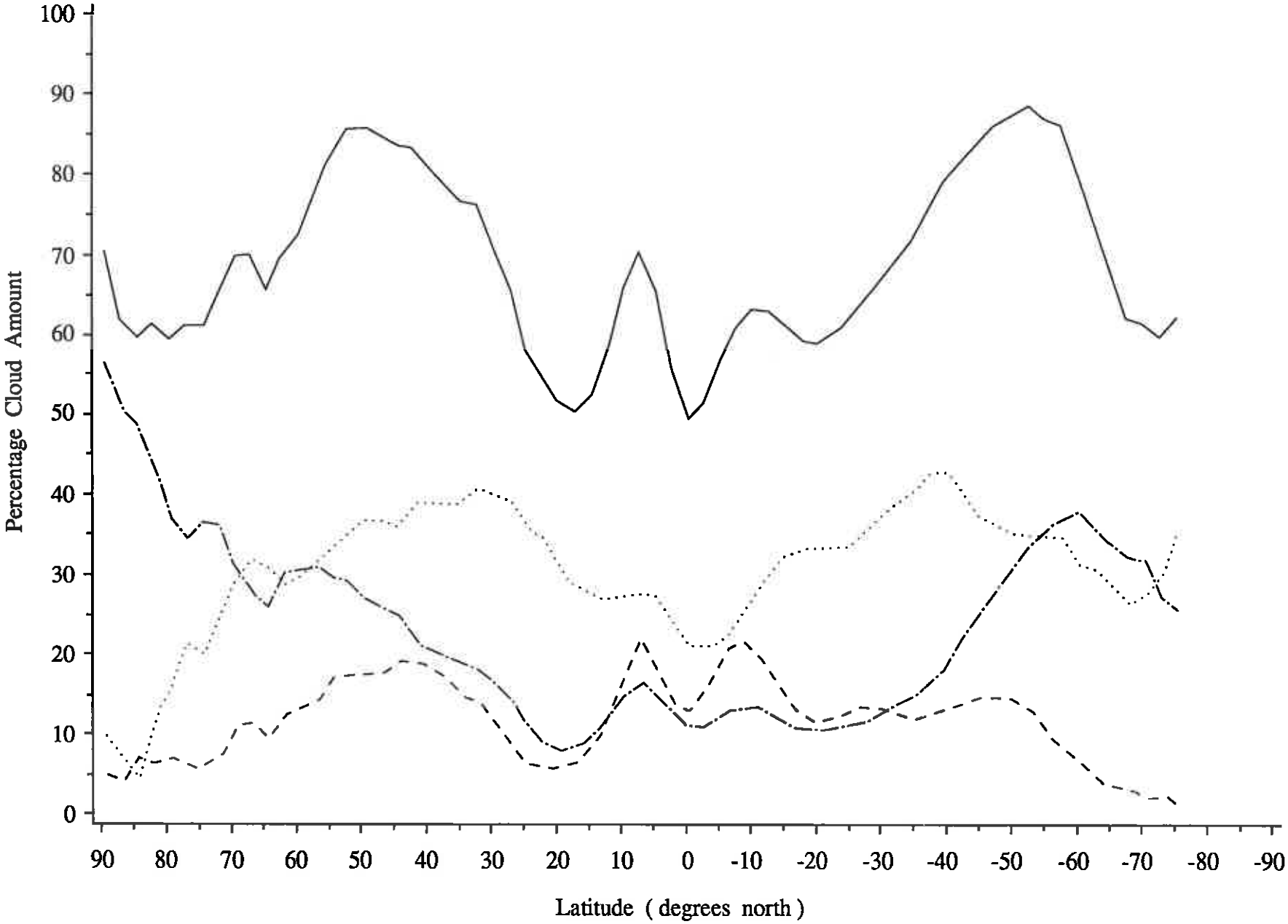
Percentage Cloud Amount
100
90
80
70
60
50
40
30
20
10
0
90 80 70 60 50 40 30 20 10 0 -10 -20 -30 -40 -50 -60 -70 -80 -90
Latitude (degrees north)

Figure 6(a)

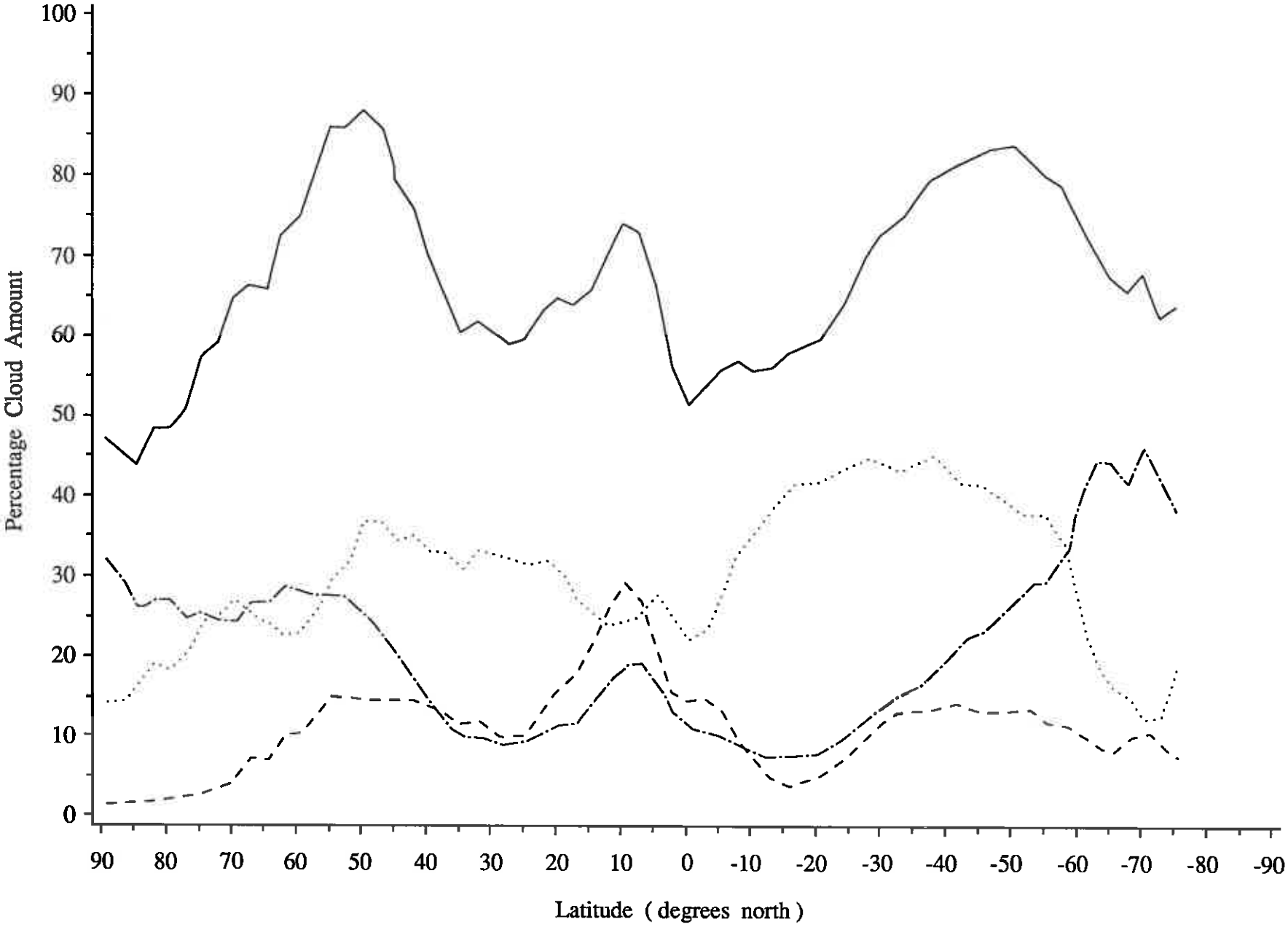
Percentage Cloud Amount
100
90
80
70
60
50
40
30
20
10
0
90 80 70 60 50 40 30 20 10 0 -10 -20 -30 -40 -50 -60 -70 -80 -90
Latitude (degrees north)

Figure 6(b)

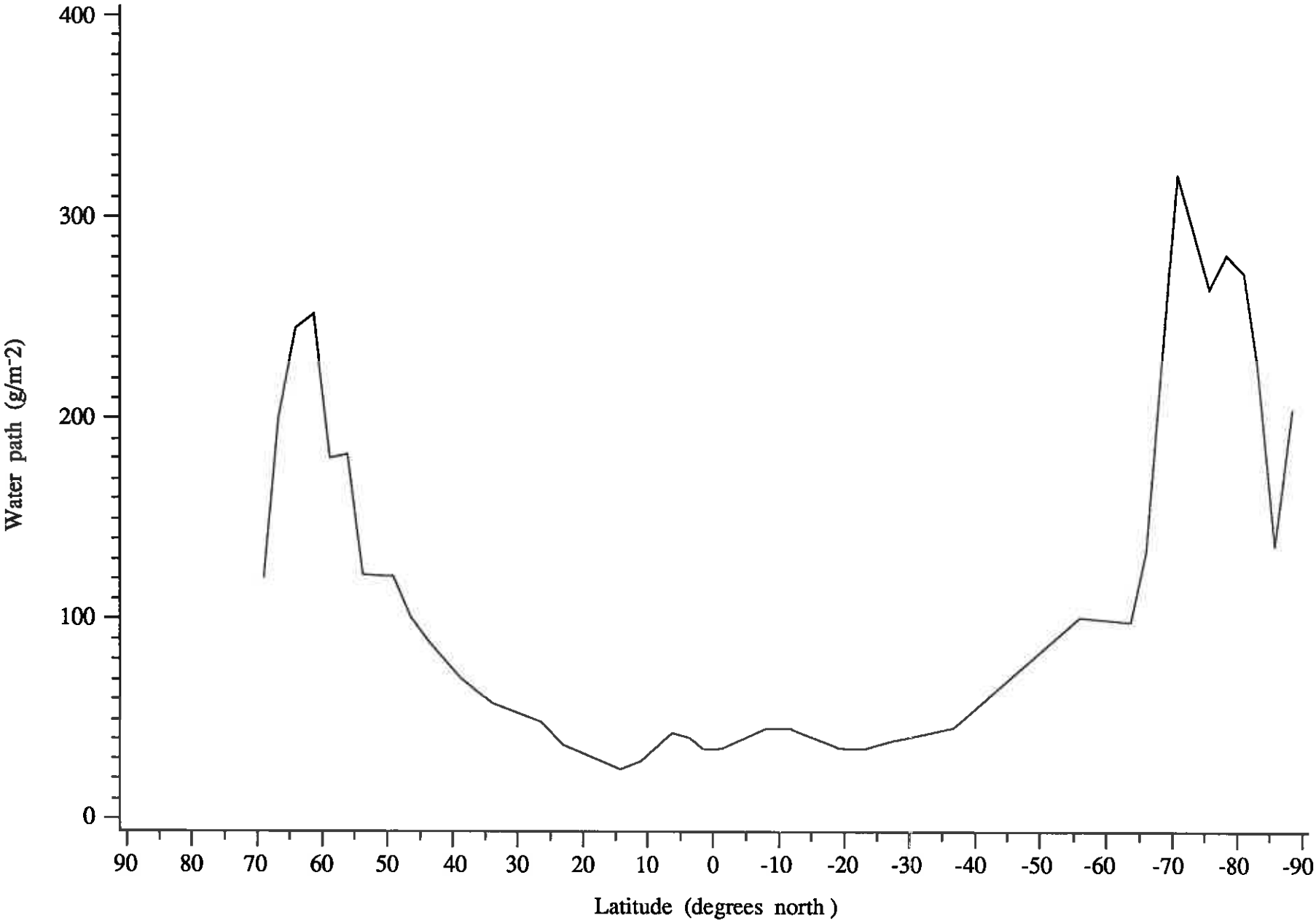
400
300
200
100
0
Water path (g/m-2)
90
80
70
60
50
40
30
20
10
0
-10
-20
-30
-40
-50
-60
-70
-80
-90
Latitude (degrees north)

Figure 7(a)

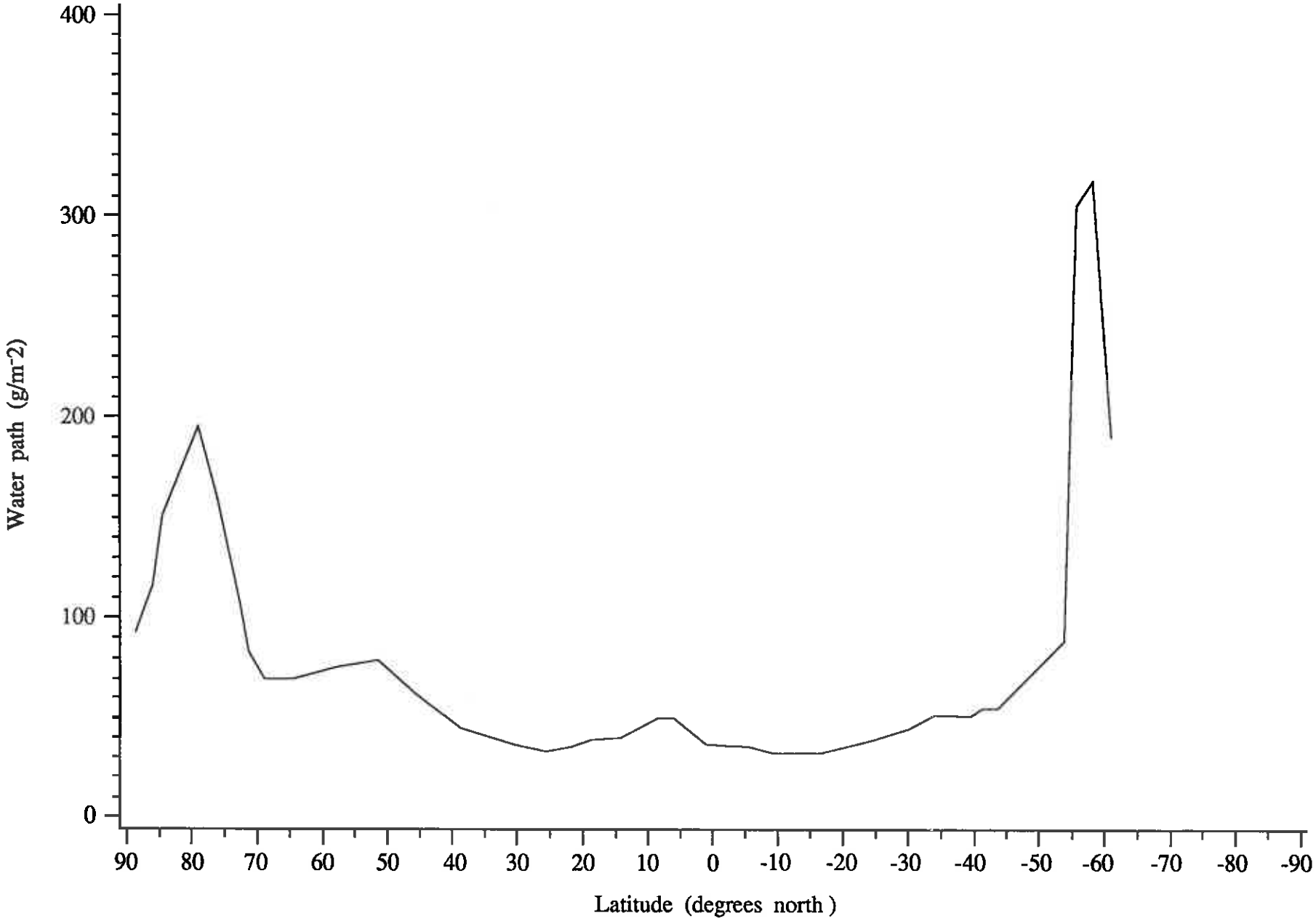
400
300
200
100
0
Water path (g/m-2)
90
80
70
60
50
40
30
20
10
0
-10
-20
-30
-40
-50
-60
-70
-80
-90
Latitude (degrees north)

Figure 7(b)

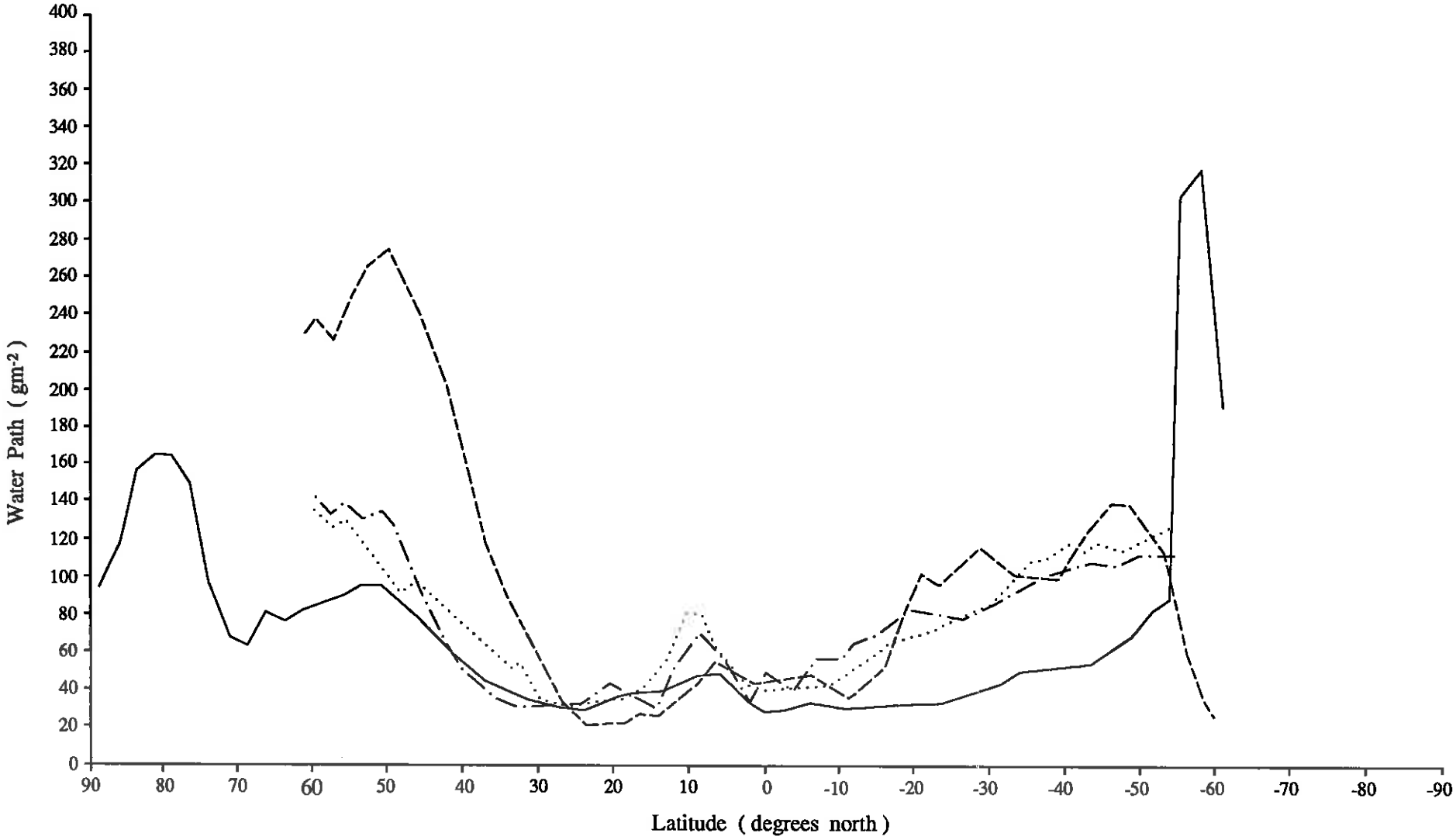
Water Path (gm-2)
400
380
360
340
320
300
280
260
240
220
200
180
160
140
120
100
80
60
40
20
0
90
80
70
60
50
40
30
20
10
0
-10
-20
-30
-40
-50
-60
-70
-80
-90
Latitude (degrees north)

Figure 8

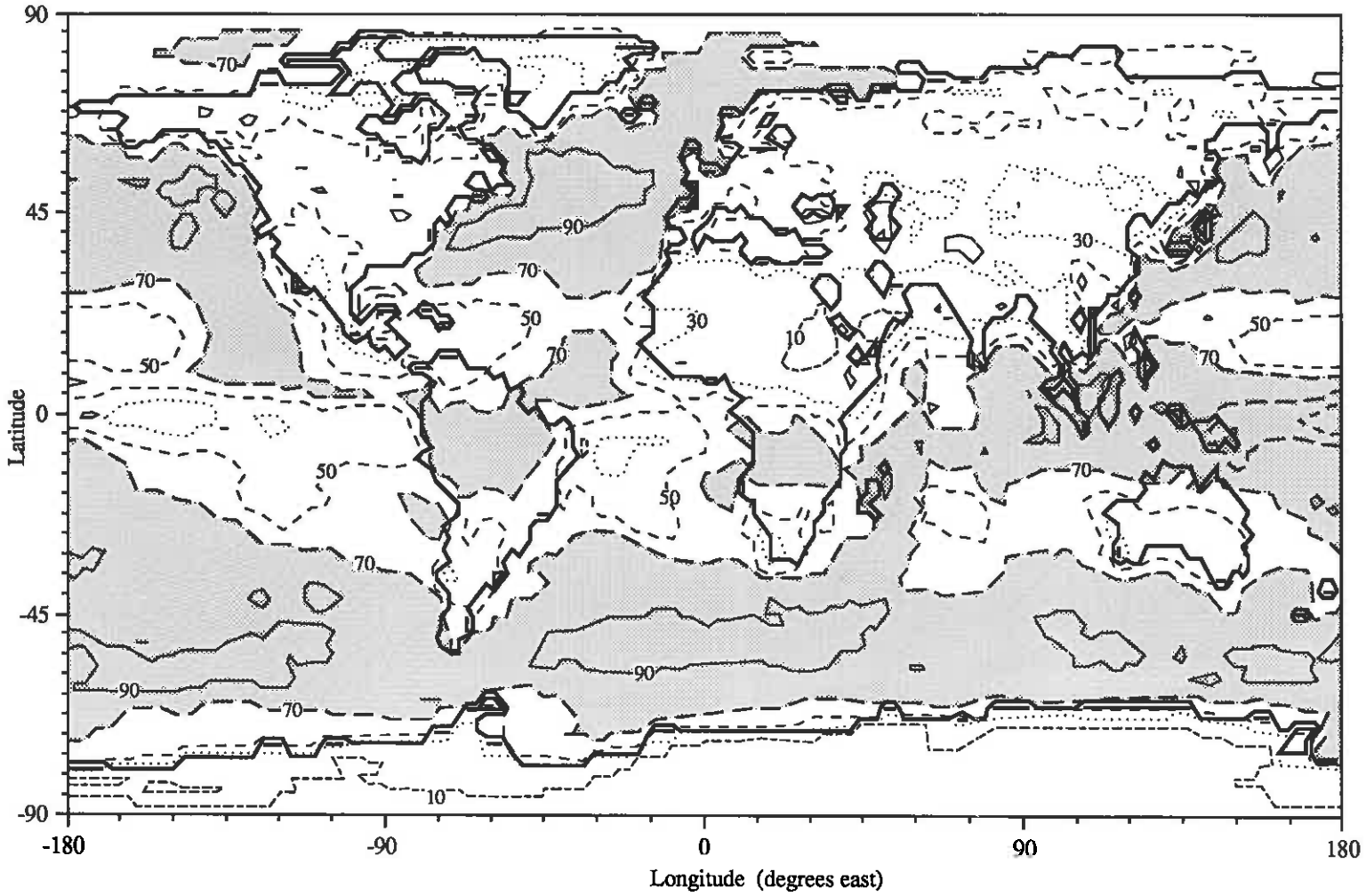
90
45
0
-45
-90
Latitude
-180
-90
0
90
180
Longitude (degrees east)
70
90
50
30
10

Figure 9(a)

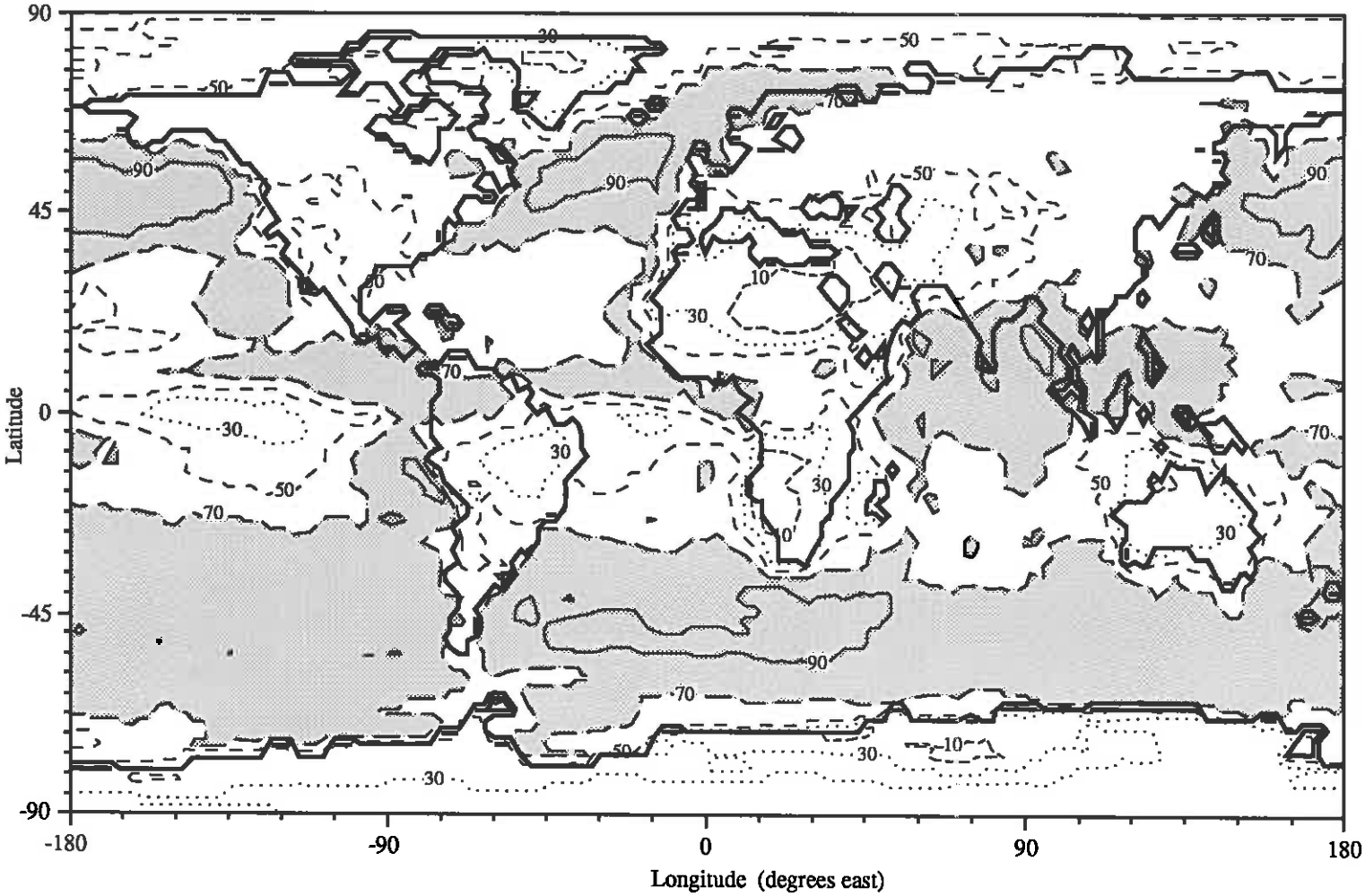

Figure 9(b)

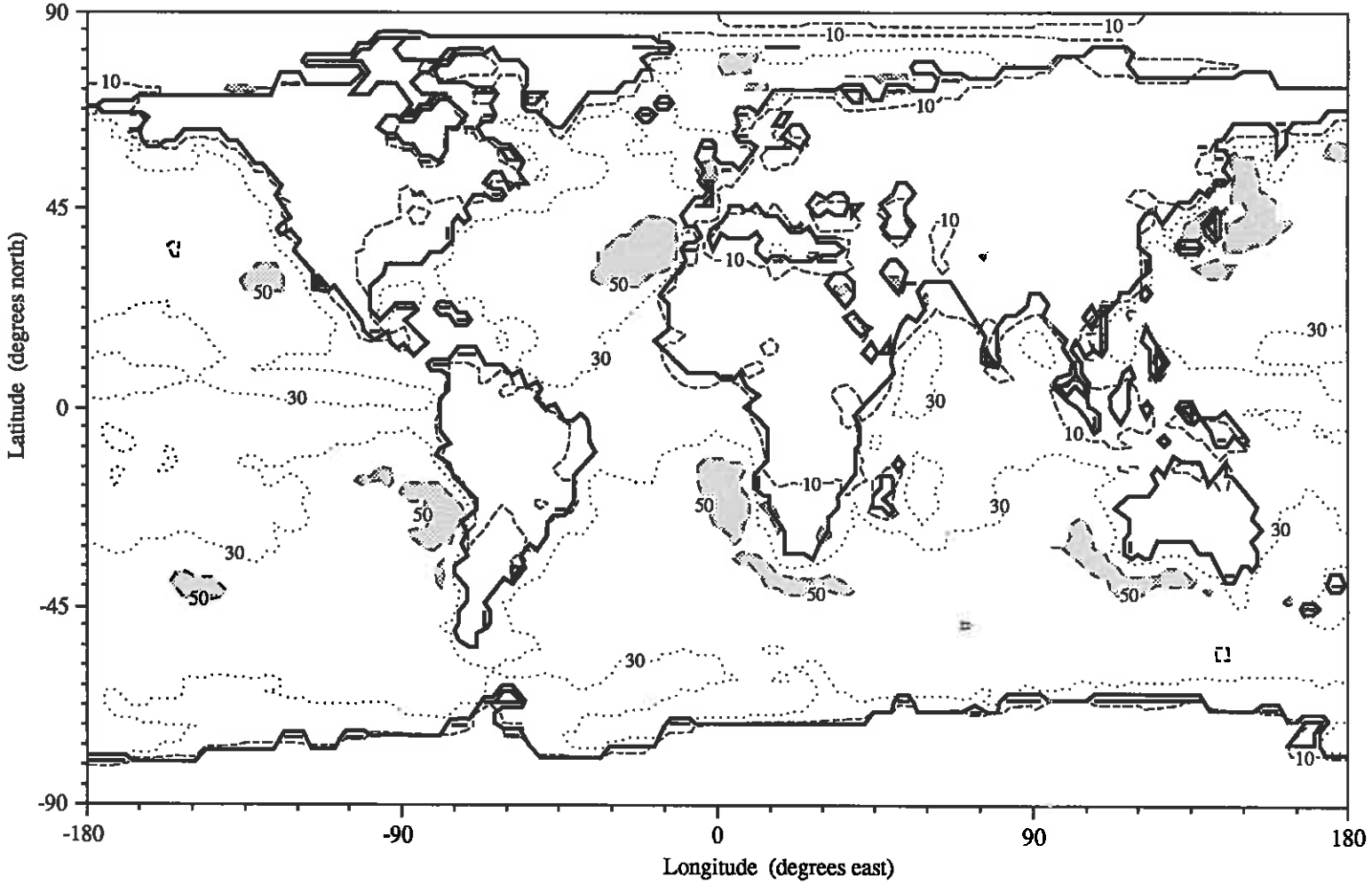
90
45
0
-45
-90
Latitude (degrees north)
-180
-90
0
90
180
Longitude (degrees east)
10
30
50

Figure 10(a)

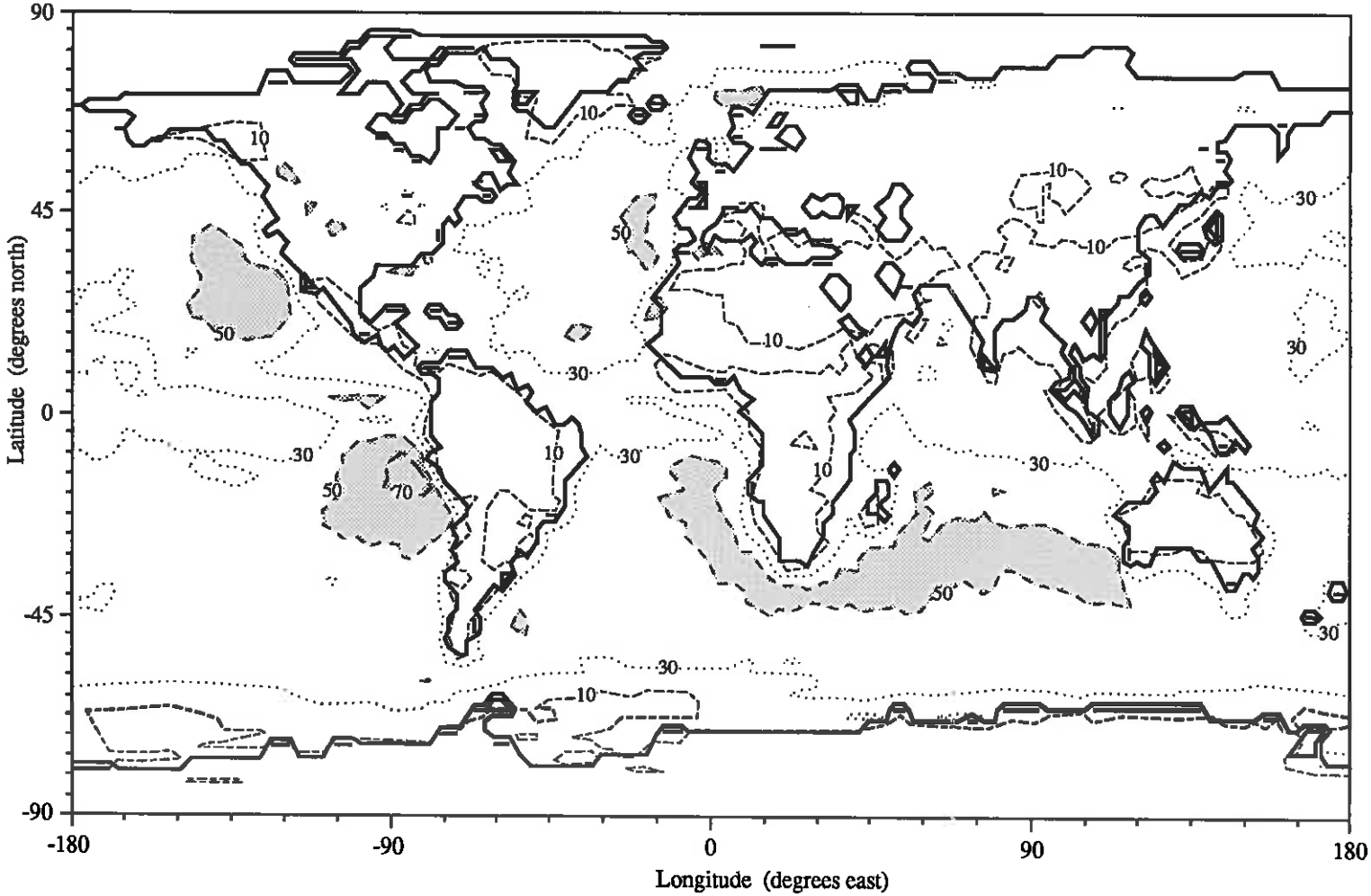
90
45
0
-45
-90
Latitude (degrees north)
-180
-90
0
90
180
Longitude (degrees east)
10
30
50
70

Figure 10(b)

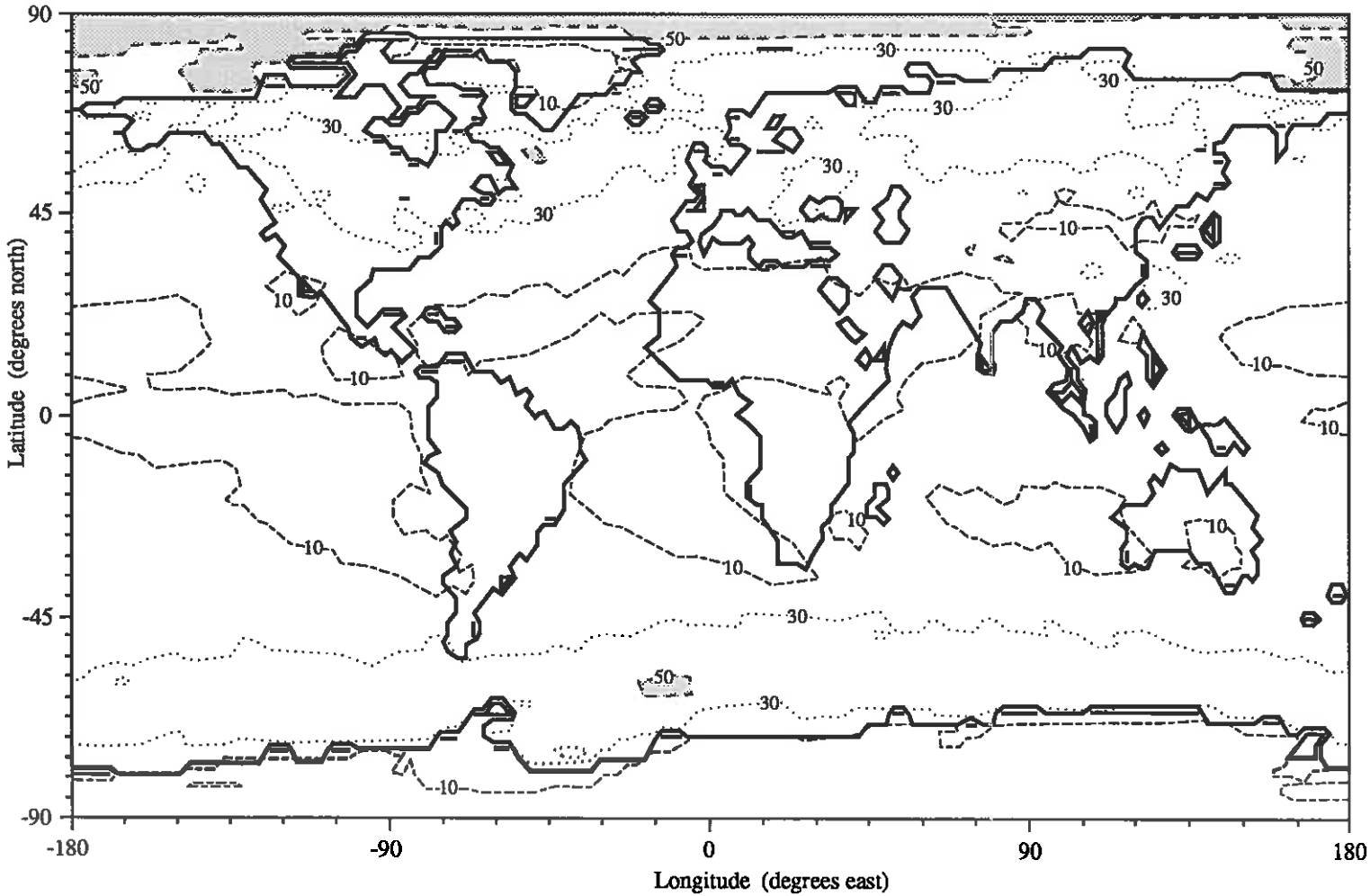
90
45
0
-45
-90
Latitude (degrees north)
-180
-90
0
90
180
Longitude (degrees east)
50
30
10

Figure 11(a)

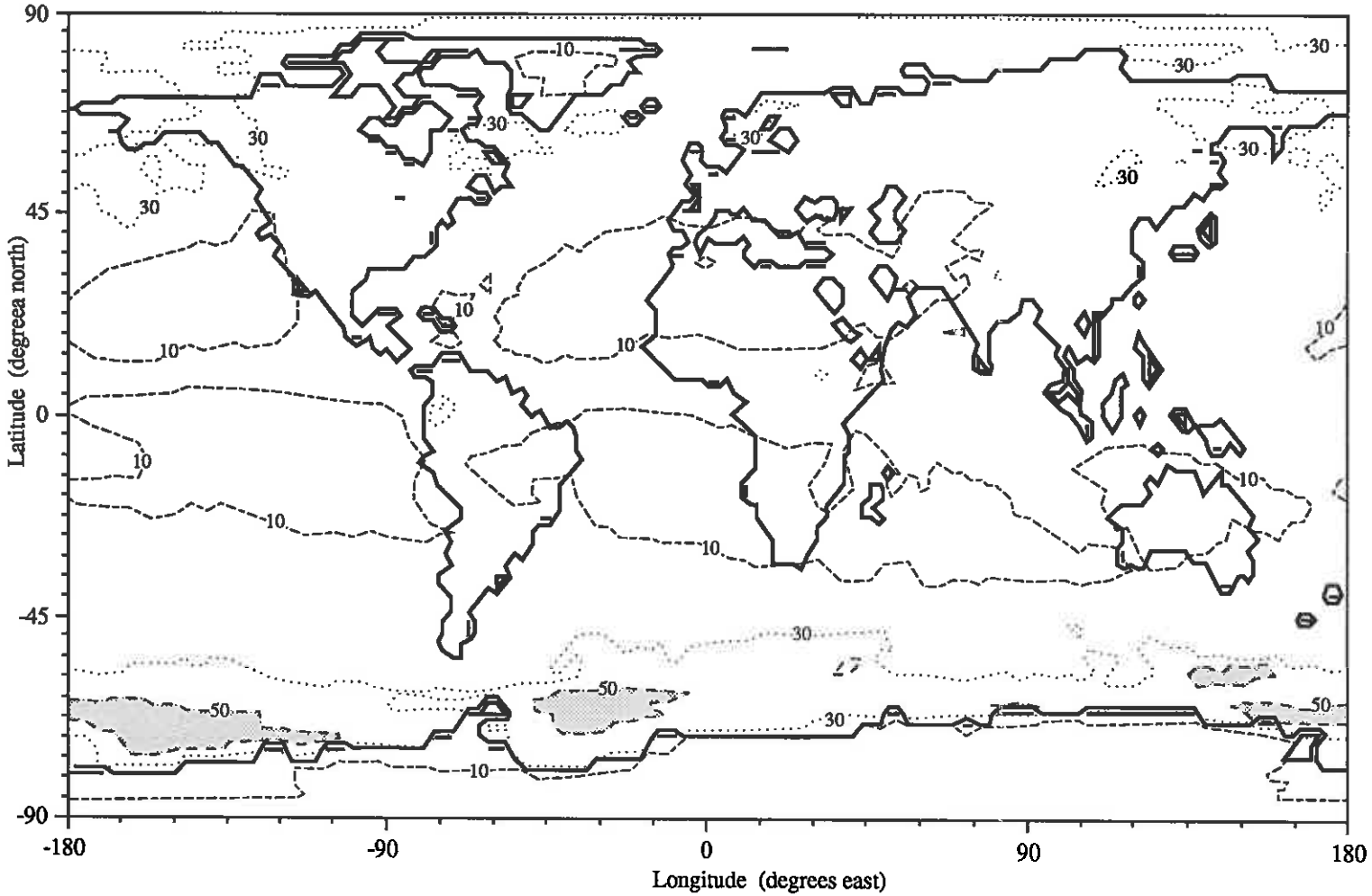
90
45
0
-45
-90
Latitude (degreea north)
-180
-90
0
90
180
Longitude (degrees east)
10
30
50

Figure 11(b)

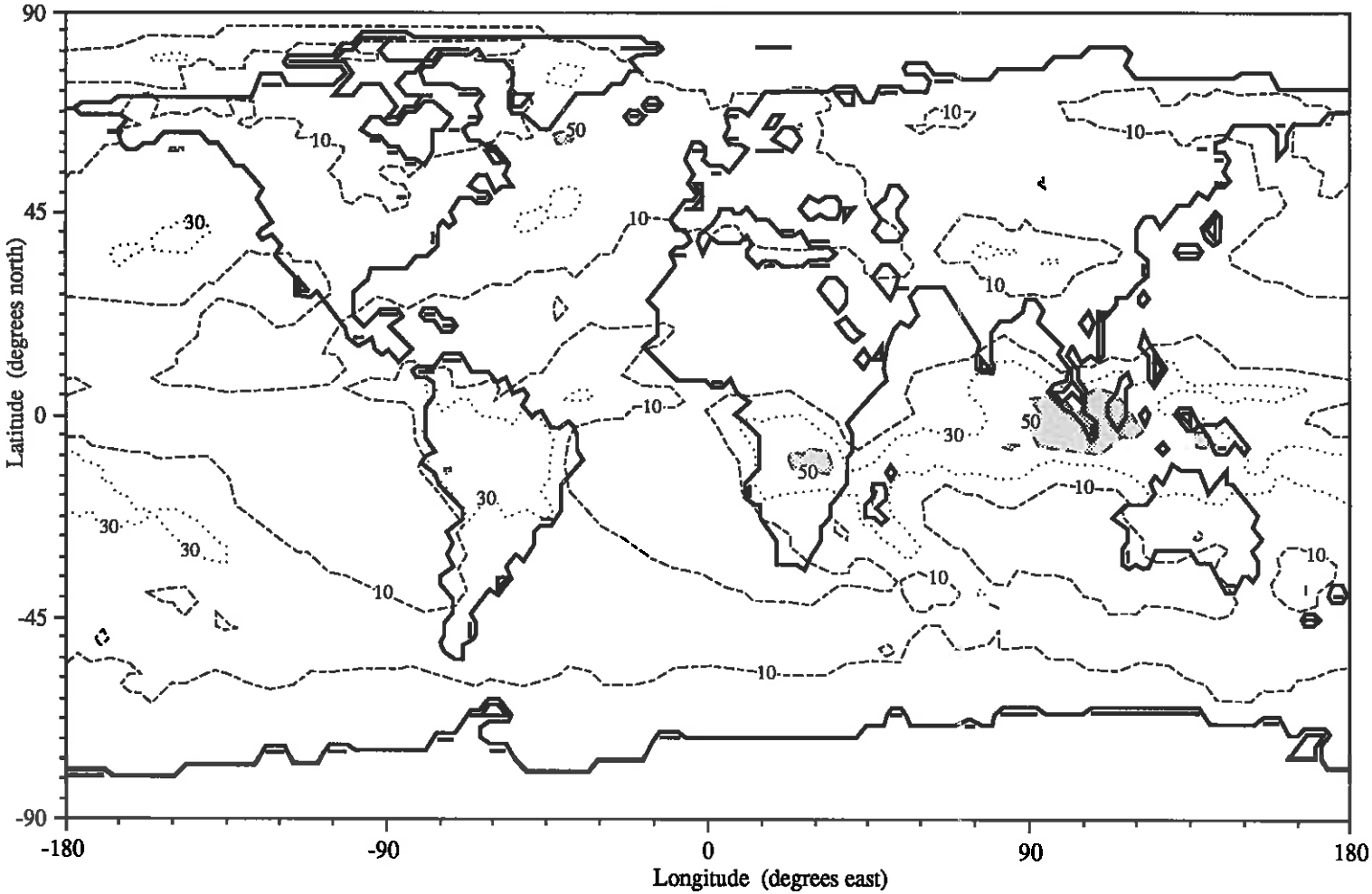
90
45
0
-45
-90
Latitude (degrees north)
-180
-90
0
90
180
Longitude (degrees east)
10
30
50

Figure 12(a)

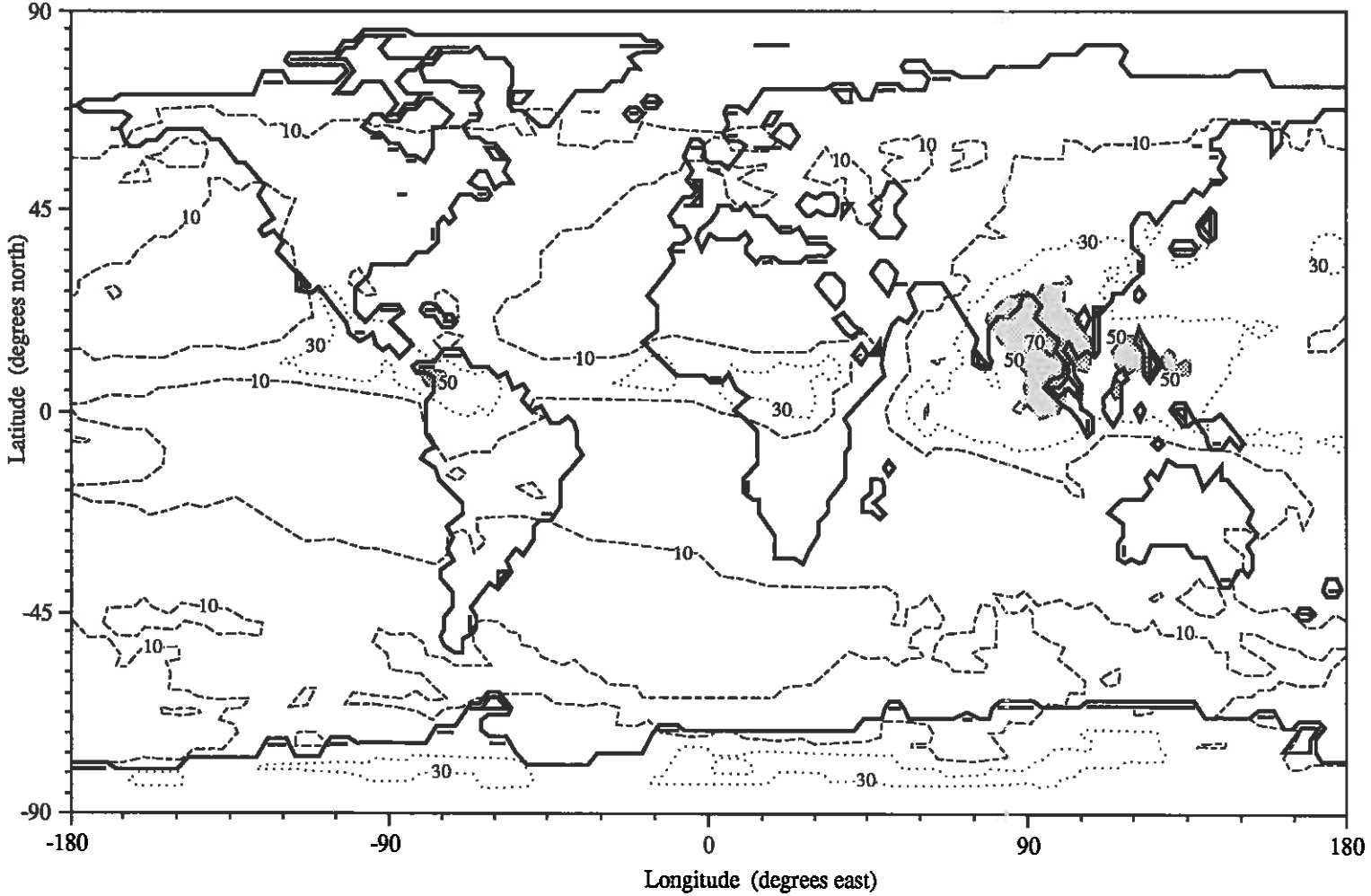
90
45
0
-45
-90
Latitude (degrees north)
-180
-90
0
90
180
Longitude (degrees east)
10
30
50
70

Figure 12(b)

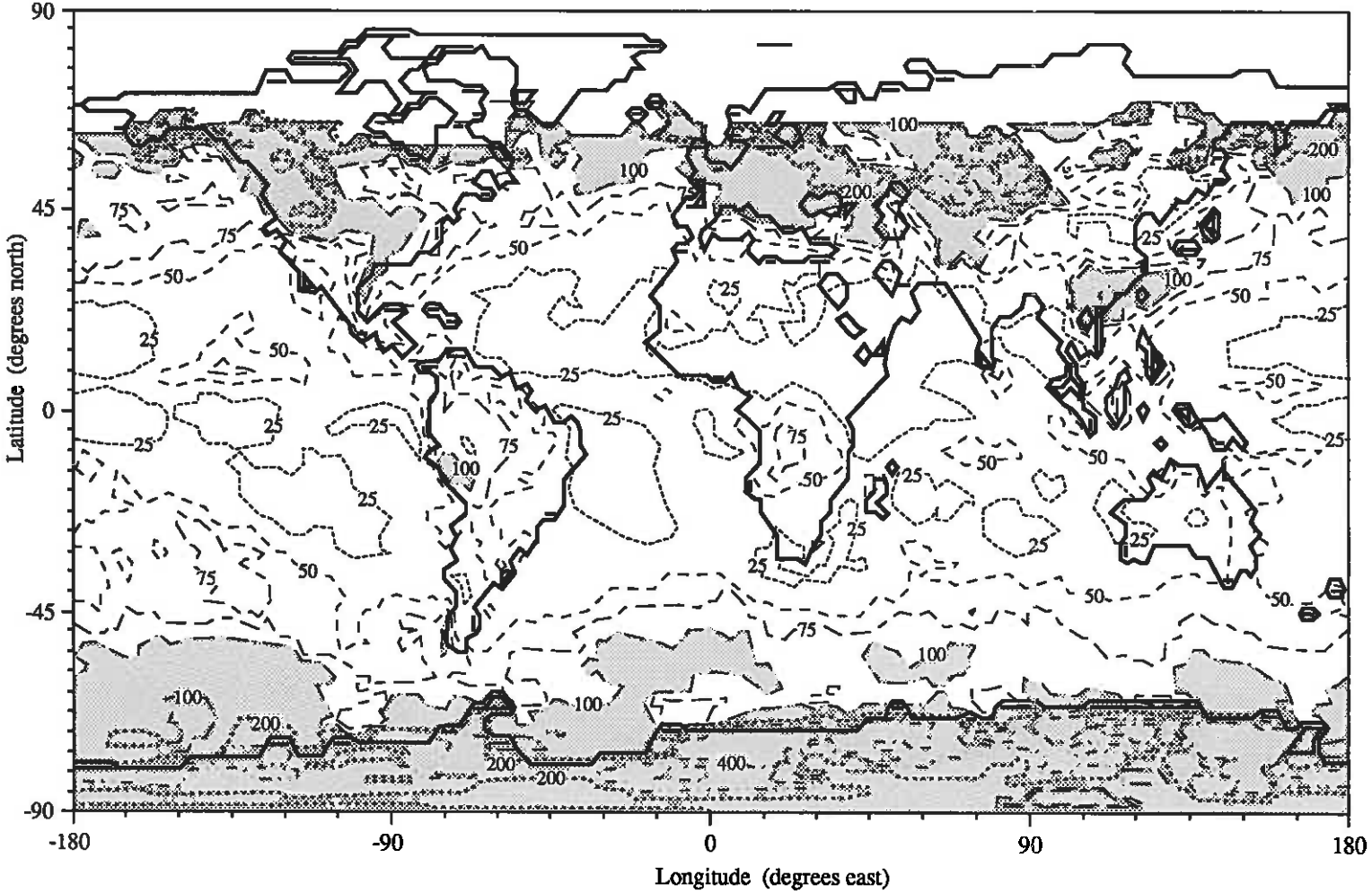
90
45
0
-45
-90
Latitude (degrees north)
-180
-90
0
90
180
Longitude (degrees east)

Figure 13(a)

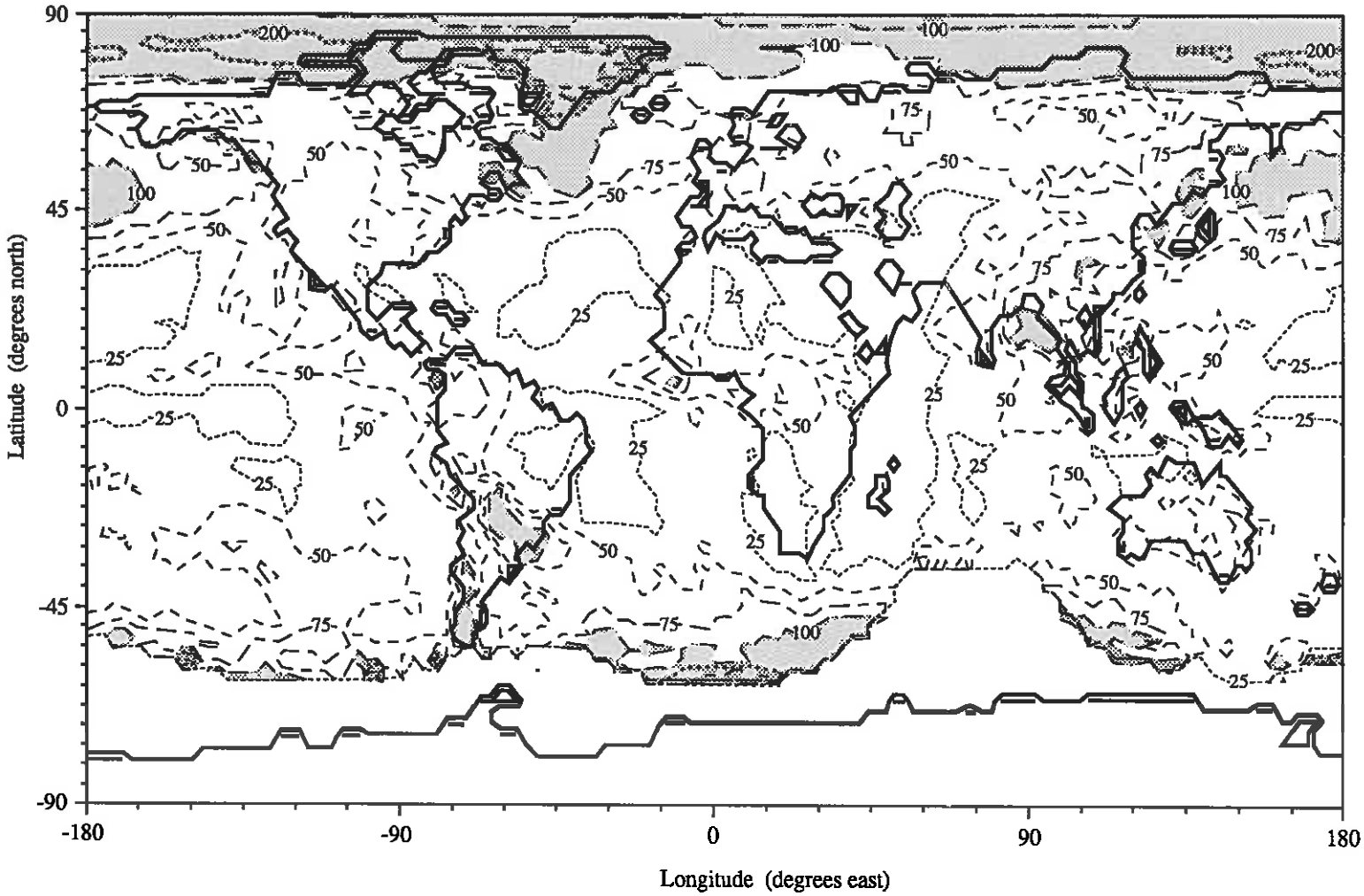
90
45
0
-45
-90
Latitude (degrees north)
-180
-90
0
90
180
Longitude (degrees east)
200
100
75
50
25

Figure 13(b)